

# MODIFICATION OF A COMMERCIAL POLY(VDF-CO-HFP) COPOLYMER LATEX

by

**Sarnia Naidoo**

Submitted in partial fulfilment of the requirements for the degree  
Master of Engineering (Chemical Engineering)

in the

Department of Chemical Engineering  
Faculty of Engineering, Built Environment and Information Technology

UNIVERSITY OF PRETORIA

August 2019

I, Sarnia Naidoo, student number 28037163, declare:

- I understand what plagiarism is and am aware of the University's policy in this regard.
- I declare that the dissertation is my own original work. Where other people's work has been used (either from a printed source, internet or any other source), this has been properly acknowledged and referenced in accordance with departmental requirements.
- I have not used another student's past written work to hand in as my own.
- I have not allowed, and will not allow, anyone to copy my work with the intention of passing it off as his or her own work.

# SYNOPSIS

---

## MODIFICATION OF A COMMERCIAL POLY(VDF-CO-HFP) COPOLYMER LATEX

Supervisor: Prof. Philip Crouse  
Co-supervisor: Dr Gerard Puts  
Department: Chemical Engineering  
University: University of Pretoria  
Degree: Master of Engineering (Chemical Engineering)  
Keywords: Fluoropolymer, poly(VDF-*co*-HFP) copolymer, latex, core-shell, emulsion polymerisation

Fluorinated polymers are niche macromolecules that play an essential role in modern life. The special properties of fluorine, including among others, a large electronegativity (*ca* 3.98), low polarisability, small van der Waal's radius (135 pm) and the strong C-F bond (*ca* 485 kJ · mol<sup>-1</sup>), impart unique properties to organofluorine compounds. Fluoropolymers exhibit a combination of desirable traits, including high thermal stability, low coefficient of friction, chemical inertness, oleo- and hydrophobicity, and low surface tension. Among the fluoropolymers, polyvinylidene fluoride (PVDF), and copolymers of vinylidene fluoride (VDF) and hexafluoropropylene (HFP), have found applications in the coatings industry as the binder in exterior coatings.

The chemical inertness of poly(VDF-*co*-HFP) copolymer, however, prevents dispersion of pigments into the coating and also inhibits adhesion of the coating onto substrates. An acrylic modifier polymer is typically added to the poly(VDF-*co*-HFP) copolymer to improve the dispersion of pigments and the adhesion of the coating. This acrylic copolymer is physically blended with the poly(VDF-*co*-HFP) copolymer on a macromolecular scale (*i.e.* it forms a thermodynamically miscible blend). The loading of acrylic copolymer in commercial PVDF coatings is often in the range of 20 to 30 % by weight of polymer solids. Typically, copolymers of methyl methacrylate, ethyl acrylate and methacrylic esters are employed.

Alternative strategies to overcome the adhesion problem include, among others, chemical modification of the surface of the fluoropolymer film. This can be achieved by graft copolymerisation or core shell emulsion polymerisation. These methods are used to func-

tionalise the polymer chains, while maintaining the desirable properties of the parent polymer. Due to environmental regulations, industry focus has shifted towards developing coatings with a low volatile organic compound (VOC) content. Aqueous, low VOC, air-drying coatings can be formulated directly from the acrylic modified fluoropolymer (AMF) latex and have superior properties to solvent based, high VOC, air-dry coatings. Their advantages include low viscosities, reduced flammability, reduced odour and easy application using conventional equipment. A large portion of the aqueous coatings are sold into the architectural market with over 70 % of architectural paints used in the United States being classified as aqueous.

Arkema Inc. has developed a commercial aqueous fluoropolymer latex using the method of seeded emulsion polymerisation. VDF and HFP monomers are randomly copolymerised *via* emulsion polymerisation. This poly(VDF-*co*-HFP) copolymer may be used as the seed material in a core-shell polymerisation using acrylic monomers. Kato *et al.* [49] discloses the preparation of an AMF formulation for poly(VDF-*co*-HFP) copolymer. Preliminary testing of membrane textiles coated with such formulations showed that the AMF coatings degrade under UV irradiation more rapidly than is expected for poly(VDF-*co*-HFP) copolymer. The patent indicates that the nature of the product formed by the emulsion polymerisation is not well understood and the product may be either a graft copolymer or a core-shell system.

The aim of this research reported in this dissertation was to shed light on the nature of the final product, and to verify the claims made in the above-mentioned patent.

Various acrylic monomers were copolymerised *via* seeded emulsion polymerisation using commercial poly(VDF-*co*-HFP) copolymer as the seed material. The concentration and the ratios of the monomers were varied according to the formulation guidelines in Kato *et al.*[49]. ATR-FTIR spectroscopy and <sup>19</sup>F NMR spectroscopy was used to determine the microstructure of the resultant latexes. ATR-FTIR spectra confirmed the presence of C=C and C=O bonds in latexes. This indicates that unreacted acrylic components are present. The ATR-FTIR spectra of the films indicated the disappearance of the C=C bonds from the latex, which indicates that the monomers are evaporated easily from the latexes during film formation. The <sup>19</sup>F NMR spectra confirmed that no modification of the poly(VDF-*co*-HFP) copolymer backbone took place during the reactions. The particle size distribution graphs showed an increase in particle sizes and this suggested that some self polymerisation of the monomer occurred. The viscosity of the latexes were lower compared to the due to the experiments being conducted under dilution.

The flow characteristics of the poly(VDF-*co*-HFP) copolymer was also influenced with some reactions yielding shear thickening latexes as compared to the shear thinning poly(VDF-*co*-HFP) copolymer. The reactions also yielded latexes which displayed lower and higher surface tensions than the poly(VDF-*co*-HFP) copolymer.

Therefore, the conclusion may be drawn from this work that core-shell formation oc-

curred during the emulsion copolymerisation, as opposed to grafting of the monomer onto the poly(VDF-*co*-HFP) copolymer backbone. The claims made in the literature could not be substantiated; in particular, the reported improvements in film forming ability were not realised. No commercially useful advantage exists for the emulsion copolymerisation of poly(VDF-*co*-HFP) copolymer with acrylic monomers over the solution blending of poly(VDF-*co*-HFP) copolymer with acrylic copolymers.

# Contents

<b>1</b>	<b>Introduction</b>	<b>1</b>
<b>2</b>	<b>Literature study</b>	<b>4</b>
2.1	Introduction . . . . .	4
2.1.1	Chemistry of fluorine . . . . .	4
2.1.2	Fluoropolymers . . . . .	5
2.1.3	Summary of properties and applications of the different fluoropolymers . . . . .	6
2.2	Fluoropolymer coatings . . . . .	7
2.2.1	Coating composition . . . . .	7
2.2.2	Solvent types . . . . .	8
2.3	Polymerisation methods . . . . .	9
2.3.1	Emulsion polymerisation . . . . .	9
2.3.2	Suspension polymerisation . . . . .	10
2.3.3	Solution polymerisation . . . . .	11
2.4	Homopolymerisation of VDF . . . . .	11
2.5	PVDF properties . . . . .	12
2.6	Copolymerisation of VDF . . . . .	13
2.6.1	Poly(VDF- <i>co</i> -HFP) copolymer . . . . .	13
2.7	Acrylic modified fluoropolymers . . . . .	13
2.8	Modification of PVDF copolymers . . . . .	14
2.9	Commercial PVDF coatings . . . . .	14
2.10	Characterisation methods . . . . .	15
2.10.1	Rheology . . . . .	15
2.10.2	Surface tension . . . . .	16
<b>3</b>	<b>Characterisation of commercial poly(VDF-<i>co</i>-HFP) copolymer</b>	<b>18</b>
3.1	Introduction . . . . .	18
3.2	Experimental . . . . .	18
3.2.1	Materials . . . . .	18
3.2.2	Methods . . . . .	19

3.2.3	Light microscopy . . . . .	19
3.2.4	Rheology . . . . .	21
3.3	Results and discussion . . . . .	21
3.3.1	Structure and composition of the polymers . . . . .	24
3.3.2	Particle size and morphology . . . . .	26
3.3.3	Flow properties . . . . .	27
3.4	Conclusions . . . . .	28
<b>4</b>	<b>Modification of poly(VDF-<i>co</i>-HFP) copolymer</b>	<b>29</b>
4.1	Introduction . . . . .	29
4.2	Experimental . . . . .	29
4.2.1	Materials . . . . .	29
4.2.2	Methods . . . . .	30
4.3	Results and discussion . . . . .	32
4.3.1	Particle size distribution, viscosity, density and surface tension . . . . .	33
4.3.2	Structure and composition of the polymers . . . . .	35
4.3.3	DSC calorimetry . . . . .	38
4.3.4	Adhesion and peel test . . . . .	39
4.4	Challenges . . . . .	41
4.5	Conclusion . . . . .	41
<b>5</b>	<b>Conclusion</b>	<b>43</b>
5.1	Summary of results . . . . .	43
5.1.1	Characterisation of commercial poly(VDF- <i>co</i> -HFP) . . . . .	43
5.1.2	Modification of poly(VDF- <i>co</i> -HFP) copolymer . . . . .	43
5.2	Suggestion for further work . . . . .	44
	<b>References</b>	<b>45</b>

# List of abbreviations

## Monomers

VDF	Vinylidene fluoride
HFP	Hexafluoropropylene
MMA	Methyl methacrylate
MA	Methacrylic acid
S	Styrene
NBA	n-Butyl acrylate
EA	Ethyl acrylate
AA	Acrylic acid

## Solvents

DMSO	Dimethylsulfoxide
DMF	Dimethylformamide
THF	Tetrahydrofuran

## Surfactants

SDS	Sodium dodecyl sulfate
-----	------------------------

## Initiators

SPS	Sodium persulfate
-----	-------------------

## Analytical techniques

NMR	Nuclear magnetic resonance
FTIR	Fourier transform infra-red
ATR	Attenuated total reflectance
DSC	Differential scanning calorimetry
PSD	Particle size distribution

## Technical terms

UV	Ultraviolet light
VOC	Low volatile organic content
AMF	Acrylic modified fluoropolymer
PVDF	Poly(vinylidene fluoride)
ETFE	Poly(ethylene- <i>alt</i> -tetrafluoroethylene)
PVF	Poly(vinyl fluoride)
PTFE	Poly(tetrafluoroethylene)
PFA	Perfluoroalkoxy alkanes
FEP	Fluorinated ethylene propylene

## Institutional abbreviations

NRF	South African National Research Foundation
FEI	Fluorochemical Expansion Initiative

## Research outputs

Publications in peer-reviewed journals:

1. Naidoo, S., Puts, G., and Crouse, P. L. **2019.**, Modification of a commercial poly(VDF-co-HFP) latex, *European Polymer Journal*, submitted August 2019.

Conference contributions:

1. Naidoo, S., Rolfes, H., and Crouse, P. L. **July 2014.**, Acrylic modified fluoropolymer latexes for coating applications, International Conference on Chemical Thermodynamics and the SAIChE National Conference, Durban, South Africa.
2. Naidoo, S., Rolfes, H., and Crouse, P. L. **December 2013.**, Benchmark Characterisation of Kynar Aquatec FMA-12, 41st National Convention of the South African Chemical Institute, East London, South Africa.

# Chapter 1

## Introduction

Fluorinated polymers are niche macromolecules that play an essential role in modern life [1]. The special properties of fluorine, including among others, a large electronegativity (*ca* 3.98) [2], low polarisability [3], small van der Waal's radius (135 pm) [4] and the strong C-F bond (*ca* 485 kJ · mol<sup>-1</sup>), impart unique properties to organofluorine compounds. Fluoropolymers exhibit a combination of desirable traits, including, high thermal stability, low coefficient of friction, chemical inertness, oleo- and hydrophobicity, and low surface tension [5–16]. Their applications span engineering thermoplastics and elastomers for the chemical process-, automotive- and aeronautics industries, weather-proof coatings, biomedical materials, separators, electrolytes, and binders for Li-batteries, exchange membranes in fuel cells, and many more [10, 17–22].

Among the fluoropolymers, poly(vinylidene fluoride) (PVDF), and copolymers of vinylidene fluoride (VDF) with hexafluoropropylene (HFP), have found special applications in the coatings industry as the binder in exterior-use coatings [23, 24]. The alternating CF<sub>2</sub> and CH<sub>2</sub> groups in PVDF induces a chain polarity that provides resistance to thermal- and UV degradation [10]. The incorporation of HFP into a PVDF chain increases the fluorine content of the polymer making poly(VDF-*co*-HFP) copolymer more hydrophobic than PVDF homopolymer [25]. Additionally, the bulky CF<sub>3</sub> pendant group imparts amorphicity to poly(VDF-*co*-HFP) copolymer.

Architectural membranes find increasing use in the construction of public spaces due to several factors, most notably the ability of these membranes to transmit light. This feature is attractive in an environmental context as efficient natural lighting of public buildings reduces day-time electricity consumption and, thereby, reduces the operating costs and environmental impact of such spaces. South Africa presents a materials challenge for these membranes as the material of construction must be able to withstand intense and prolonged UV irradiation. Poly(ethylene-*alt*-tetrafluoroethylene) (ETFE), PVDF and poly(VDF-*co*-HFP) are excellent choices for UV resistant membrane materials. However, these polymers are expensive and a more cost effective approach involves the coating of cheaper textiles with a UV resistant fluoropolymer coating.

The chemical inertness of poly(VDF-*co*-HFP) copolymer, however, prevents dispersion of pigments into the coating and also inhibits adhesion of the coating onto substrates [10, 15, 24]. An acrylic modifier polymer is typically added to the poly(VDF-*co*-HFP) copolymer to improve the dispersion of pigments and the adhesion of the coating. This acrylic copolymer is physically blended with the poly(VDF-*co*-HFP) copolymer on a macromolecular scale (*i.e.* it forms a thermodynamically miscible blend [10, 23, 24]). The acrylic copolymer, typically copolymers of methyl methacrylate, ethyl acrylate and methacrylic esters, in commercial PVDF coatings is often in the range of 20 to 30 % by weight of polymer solids [26, 27].

Chemical modification of the surface of the fluoropolymer film is one strategy, among others, to overcome the adhesion problem. This can be achieved by graft copolymerisation [28–31] or core-shell emulsion polymerisation. These methods are used to functionalise the polymer chains, but also maintains the desirable properties of the parent polymer.

Poly(VDF-*co*-HFP) copolymers may undergo graft copolymerisation at the  $\text{CF}_2-\text{CH}_2-\text{CF}_2$  position [32]. The wettability, surface tension and adhesion properties of the polymer may be tailored *via* grafting by selecting some suitable graft monomer [33].

Core-shell particles have received much attention in the literature as their properties may be finely tuned [34, 35]. They exhibit superior properties as compared to particles produced by physically blending of polymers and particles produced by random copolymerisation (*i.e.* excellent film formation, hardness, appearance, and block resistance) [36]. These core-shell particles are prepared by a series of emulsion polymerisation steps [37]. During the first step, the (co)monomers for the core (co)polymer are (co)polymerised and then used as seed particles in the second stage of polymerisation. The shell (co)polymer is produced by (co)polymerisation of (co)monomers in the presence of the core (co)polymer seed particles [38–42], which results in physical coating of the core particle by the shell (co)polymer. Importantly, no grafting of the shell (co)polymer onto the core (co)polymer takes place.

Due to environmental regulations, industry focus has shifted towards developing coatings with a low volatile organic content (VOC) [43–46]. Aqueous, low VOC, air-drying coatings can be formulated directly from the acrylic modified fluoropolymer (AMF) latex. These aqueous coatings have superior properties compared to solvent based coatings [24], such as: low viscosity, reduced flammability, reduced odour and easy application using conventional equipment [47]. A large portion of the aqueous coatings are sold into the architectural market with over 70 % of architectural paints used in the United States being classified as aqueous [48].

Arkema Inc. has developed a commercial aqueous fluoropolymer latex using the method of seeded emulsion polymerisation. VDF and HFP monomers are randomly copolymerised *via* emulsion polymerisation. This poly(VDF-*co*-HFP) copolymer may be used as the seed material in a core-shell polymerisation using acrylic monomers [24].

Kato *et al.*[49] discloses the preparation of an AMF formulation for poly(VDF-*co*-HFP) copolymer. Preliminary testing of membrane textiles coated with such formulations showed that the AMF coatings degrade under UV irradiation more rapidly than what is expected for poly(VDF-*co*-HFP) copolymer. The patent [49] indicates that the nature of the product formed by the emulsion polymerisation is not well understood and the product may be either a graft copolymer or a core-shell system.

Knowledge of the microstructure of the AMF material is especially important in a South African context as the commercial viability of any project seeking to use AMF based architectural membranes depends strongly on the cost-effectiveness of such membranes and said cost-effectiveness is intimately tied to the expected lifetime of the AMF coated membrane. The purpose of this work was to reproduce the poly(VDF-*co*-HFP) copolymer based AMF material and ascertain the nature of the product (graft copolymer or core-shell copolymer) as well as the film forming ability. Emphasis is placed on determining if the less-than-satisfactory UV stability can be overcome or if this stability issue is inherent to the structure of the AMF.

The poly(VDF-*co*-HFP) copolymer was not synthesised in this study and the investigation is limited only to the emulsion copolymerisation of the acrylic monomers in the presence of a commercial poly(VDF-*co*-HFP) latex.

# Chapter 2

## Literature study

### 2.1 Introduction

This chapter aims to describe the unique properties and importance of using PVDF and its copolymers with HFP as the resin in a coating. Furthermore the layout of this chapter illustrates the choice of using poly(VDF-*co*-HFP) copolymer in this study since it fulfilled the requirements of having a low VOC content and being the product of seeded emulsion polymerisation.

#### 2.1.1 Chemistry of fluorine

The name fluorine is derived from its most abundant naturally occurring compound: fluorspar ( $\text{CaF}_2$ ). Fluorine forms compounds with every other element on the periodic table except helium, argon and neon. This high reactivity of  $\text{F}_2$  can be attributed to its low dissociation energy and to the high strength of the bonds that fluorine forms with other elements [50]. Some of the typical average bond energies of the halogens are shown in Table 2.1.

**Table 2.1:** Typical bond energies ( $\text{kJ} \cdot \text{mol}^{-1}$ ) [50]

X	XX ( $\text{kJ} \cdot \text{mol}^{-1}$ )	HX ( $\text{kJ} \cdot \text{mol}^{-1}$ )	$\text{BX}_3$ ( $\text{kJ} \cdot \text{mol}^{-1}$ )	$\text{AlX}_3$ ( $\text{kJ} \cdot \text{mol}^{-1}$ )	$\text{CXX}_4$ ( $\text{kJ} \cdot \text{mol}^{-1}$ )
F	159	574	645	582	456
Cl	243	428	444	427	327
Br	193	363	368	360	272
I	151	294	272	285	239

Fluorine has the highest electronegativity and therefore can oxidize many other elements to their highest oxidation state. Due to the high oxidation potential and the small size of the fluorine molecule allows the formation of many simple and complex fluorides in

which the other elements are at their highest oxidation state [51]. Some of the properties of fluorine are shown in Table 2.2.

**Table 2.2:** Physical properties of fluorine [50]

Property	F
Atomic Number	9
Number of stable isotopes	1
Atomic Weight	18.998
Electronic Configuration	[He]2s <sup>2</sup> 2p <sup>5</sup>
Ionization Energy	1680.6 kJ · mol <sup>-1</sup>
Electron Affinity	332.6 kJ · mol <sup>-1</sup>
$\Delta H_{dissoc}$	158.8 kJ · mol <sup>-1</sup> (F <sub>2</sub> )
Ionic Radius F <sup>-</sup>	133 pm
Van der Waals Radius	135 pm
Distance F-F in F <sub>2</sub>	143 pm

### 2.1.2 Fluoropolymers

Fluoropolymers are polymers that have either all the hydrogens in their analogous hydrocarbon structures replaced by fluorine atoms (perfluorinated) or they contain both hydrogen atoms and fluorine atoms (partially fluorinated) [14]. Additionally two kinds of polymers exist: homopolymers and copolymers.

Homopolymers describe polymers whose structure can be represented by the repetition of a single type of repeat unit that may be composed of one or more species of monomer unit [52]. The structure of a homopolymer is shown in Figure 2.1. Copolymers therefore, describe polymers whose repeat units are composed of two or more different repeat unit. Types of copolymers are random copolymers (Figure 2.2), statistical copolymers, alternating copolymers (Figure 2.3), graft copolymers (Figure 2.4) and block copolymers (Figure 2.5).



**Figure 2.1:** Structure of a homopolymer [52]



**Figure 2.2:** Structure of a random copolymer [52]



**Figure 2.3:** Structure of an alternating copolymer [52]

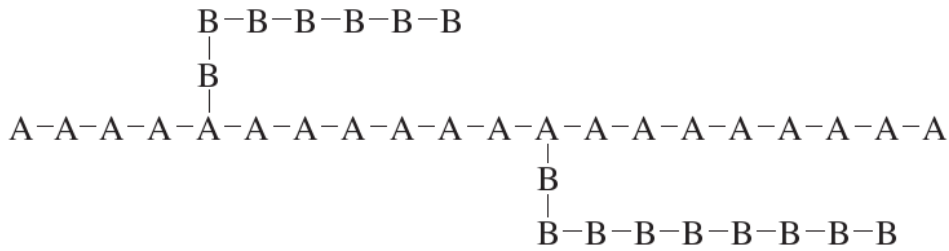


**Figure 2.4:** Structure of a graft copolymer [52]



**Figure 2.5:** Structure of a block copolymer [52]

According to the American Society for Testing Materials (ASTM), homopolymers contain 99 % or more by weight of one monomer and less than 1 % by weight of another monomer. Copolymers contain 1 % or more by weight of one or more comonomers.

Due to the strength of the fluorine-carbon bond and the high electronegativity of the fluorine atom, fluoropolymers possess many favourable properties when compared to their analogous hydrocarbon structures. Some of the properties of fluoropolymers are superior chemical resistance, weather resistance, thermal stability, low dielectric constant and low coefficient of friction, oil and water repellency and low surface tension [5–15].

### 2.1.3 Summary of properties and applications of the different fluoropolymers

Table 2.3 shows the different fluoropolymers with their applications. The fluoropolymers that are mainly used for coating applications are PVF, PTFE and PVDF. The number of fluorine atoms in each of the polymers has a significant effect on the properties of the polymer.

PVF contains only one fluorine atom and its fusion temperature and its decomposition temperature are so close that PVF can decompose upon baking when it is used as a coating [10].

PTFE has four fluorine atoms and no crystalline melting point and a high sintering point and as such forms porous surfaces. According to [10] the sintering temperature is well above the temperature that the coating can withstand before losing its mechanical

properties. Also PTFE cannot be dissolved in any solvent therefore no suitable solvent based coating can be formulated.

PVDF has alternating carbon-fluorine bonds and carbon-hydrogen bonds. This structure induces a polarity that is responsible for the resistance of dirt, oxidation, photochemical deterioration, fading, chalking, cracking and airbourne pollutants [10]. These properties make PVDF the most suitable fluoropolymer for coating applications.

**Table 2.3:** Fluoropolymers and their applications

Fluoropolymer	Application
ECTFE	Flame resistant insulation
ETFE	Wire and cable insulation
FEP	Cable insulation
PCTFE	Barrier film, packaging, sealing
PFA	Chemical resistant components
PTFE	Chemical processing, wire, coating
PVDF	Coating, wire, cable, electronics
PVF	Lamination, film, coating
THV	Barrier film, insulation

## 2.2 Fluoropolymer coatings

A coating is applied to a surface such that it adheres to the surface and forms a film. The functions of a coating can be to protect the surface as well as for decorative purposes. Some terms that are used to describe coatings by their decorative appearance are: glossy, clear, pigmented or metallic. The terms used to describe coatings by their functions are: corrosion protective, abrasion protective, skid resistant, decorative or photosensitive [53]. The terms paint and finish are synonyms for coating [54].

### 2.2.1 Coating composition

A coating is generally composed of:

- Resin (also called binders or vehicles)
- Pigment
- Additives
- Carrier

The resin is usually a polymer or polymer precursor that can be a thermoplastic or thermosetting. According to [54] a thermoplastic resin contains at least one high molecular weight polymer that provides the required mechanical strength properties without

further polymerisation. A thermosetting resin contains lower molecular weight polymers that are further polymerisation after application.

The carrier is a volatile liquid that can be either an organic solvent or water. The carrier plays a major role in the application of the coating. The solvent liquefies all the components of the coating allowing them to be spread out over the substrate [55]. Evaporation of the solvent occurs during and after application of the coating [53]. According to [53] thermoplastic resins with polymers dissolved in organic solvents have low solid content because the relatively high molecular weight requires large amounts of solvents to reduce the viscosity to allow for application.

Air pollution regulations stipulate the goal to reduce the solvent content (volatile organic compounds) of coatings. Strategies to decrease the amount of solvent in coatings include increasing the solids content of the coatings, using water as a large part of the volatile component and by eliminating the use of solvents completely.

Pigments are small insoluble particles whose purpose is to provide colour and opacity to the coating. The additives are substances that are added in small amounts to alter the properties of the coating for example the flow properties and stabilizers [53].

## 2.2.2 Solvent types

Due to environmental concerns, water based coatings are preferred over organic solvent based coatings.

### Water based coatings

Water based coatings can be manufactured from fluoropolymer dispersions or from fluoropolymer powders. Coatings from fluoropolymer dispersions are easier to make since the dispersion is the product of the emulsion polymerisation of the fluoropolymer also called a fluoropolymer latex or fluoropolymer emulsion. The typical diameter of the dispersed particles are 0.15  $\mu\text{m}$  to 0.3  $\mu\text{m}$  with the particles being spherical or rod-like in shape [55].

Aqueous dispersions display water-like viscosities and are less than 50 centipoise. Due to this low viscosity film thickness is kept low in order to avoid the problem of dripping, sagging and running [55].

There are two difficulties that are encountered with aqueous dispersion coatings. The first issue is shear stability. According to [55] most dispersions have a limited shear stability and shear is used as a method to destabilize the dispersion into a solid material to produce finer products. Something must be added to the formulation to increase the shear stability of the coating. This is usually a type of solvent [55].

The second issue is cracking of the coating as the coating is dried and baked. This is due to the small size of the dispersed particles. The cracking occurs at a low dry-film thickness and is most common in PFA and FEP dispersions [55]. An additive must be

added to minimize the cracking or to delay it to a higher dry-film thickness. An acrylic resin is usually added for this purpose. According to [55] it forms a continuous film and remains intact until the fluoropolymers melt or sinters after which it decomposes and diffuses out of the film.

## Solvent based coatings

For solvent based coatings, the fluoropolymer is almost always in the form of a powder. The exception being amorphous fluoropolymers like Teflon AF which are soluble in the solvent [55].

In order to disperse the fluoropolymer particles into the solvent, a dispersing agent is needed. This is usually a resin which stabilizes the dispersion [55].

The stability of solvent based coatings vary. If settling occurs they can be redispersed and this means that the shelf life can be up to many years [55].

Due to environmental concerns and regulations there is a need to manufacture coatings with a low volatile organic compound concentration (VOCs). Volatile organic compounds are generally flammable, toxic and are associated with a large carbon footprint. Therefore water-based fluoropolymer coatings are preferred to organic solvent based coatings.

## 2.3 Polymerisation methods

### 2.3.1 Emulsion polymerisation

Components needed for emulsion polymerisation include:

- Monomer
- Continuous phase (usually water)
- Initiator
- Surfactant

Emulsion polymerisation occurs when the monomer is insoluble in water and able to polymerise by free radicals. The initiator must be water soluble. The basis of emulsion polymerisation is the formation of micelles which are formed by the surfactant at high concentrations.

There are three stages of emulsion polymerisation:

- Stage 1: The monomer diffuses into the empty micelle. The monomer is polymerised in the micelle creating polymer particles. More polymer particles are produced as the micelles are consumed.

- Stage 2: No more surfactant is available to generate new polymer particles. The remaining monomer then diffuses into the existing number of particles to maintain equilibrium with the particle. The monomer is slowly consumed.
- Stage 3: The monomer droplets are depleted and the particle size is now constant. Conversion rate of the monomer can reach up to 80-100 %.

### **Advantages of emulsion polymerisation**

The advantages of emulsion polymerisation include good temperature control, low viscosity and the final product can be obtained in the form of a fine powder or in liquid form [56].

### **Disadvantages of emulsion polymerisation**

The disadvantage of emulsion polymerisation is due to the possibility of excess surfactant being an impurity. For example, in medical applications the excess surfactant could act as an irritant [56].

## **2.3.2 Suspension polymerisation**

The components needed for suspension polymerisation include:

- Monomer
- Continuous phase (usually water)
- Initiator
- Stabilizer

The monomer is insoluble in water and the initiator is soluble in the monomer phase. The stabilizer is often a polymer. The polymerisation occurs in a stirred tank reactor and the aim of suspension polymerisation is to obtain dispersion of monomer droplets in the aqueous phase. This dispersion must be as uniform as possible and the coalescence of the droplets during the polymerisation process must be controlled [57].

Each droplet consists of the monomer into which the initiator has been dissolved. The stabilizer is absorbed at the interface of the droplet and hinders coalescence. Each of these droplets then acts as a batch reactor whose kinetics are identical to a typical large scale free radical polymerisation.

### **Advantages of suspension polymerisation**

The advantages of suspension polymerisation include low viscosity, easy heat removal due to high heat capacity of water, and the polymerisation yields finely divided, stable latexes and dispersions that can be directly used in coatings, paints and adhesives [56].

### **Disadvantages of suspension polymerisation**

Suspension polymerisation cannot be used for polymers whose glass transition temperature is less than the polymerisation temperature since aggregation will occur [56].

## **2.3.3 Solution polymerisation**

The components needed for solution polymerisation include:

- Monomer
- Initiator
- Solvent

There are two types of solution polymerisation namely homogeneous and heterogeneous. Homogeneous solution polymerisation occurs when the polymer is soluble in the solvent as opposed to heterogeneous solution polymerisation which occurs when the polymer is insoluble in the solvent. The heterogeneous system leads to precipitation polymerisation.

### **Advantages of solution polymerisation**

The solvent acts as a diluent and aids in the removal of heat of polymerisation. It also reduces the viscosity which makes processing easier.

### **Disadvantages of solution polymerisation**

Chain transfer to the solvent occurs which results in low molecular weights. It is also difficult to remove the solvent from the final product which then leads to degradation of the bulk properties. Another disadvantage of solution polymerisation is environmental pollution which can occur due to solvent release.

## **2.4 Homopolymerisation of VDF**

The polymerisation of VDF is usually achieved through emulsion, suspension and solution processes. When compared to suspension polymerisation, emulsion polymerisation results in greater head-to-head defects. These defects influence the crystallinity which in turn

affects the mechanical strength, toughness and impact resistance of the PVDF [58]. The process of radical polymerisation of VDF is shown in Figure 2.6. Environmental concerns about the bio-accumulation of long chain fluorinated surfactants prohibit their use and alternative surfactants must be used.

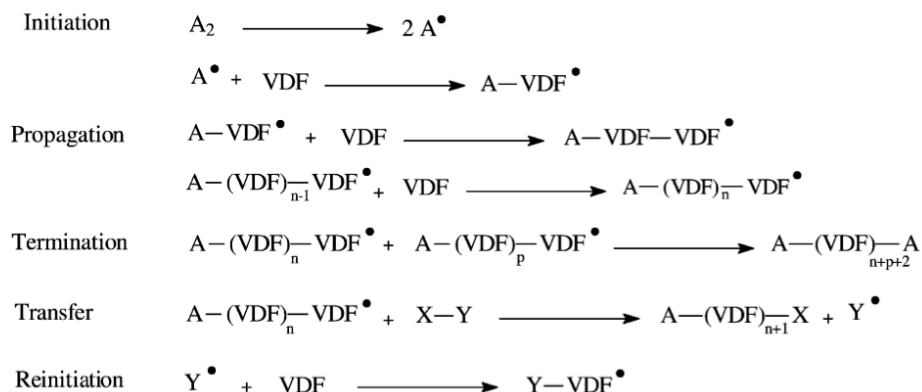


**Figure 2.6:** Reaction scheme of radical polymerisation of VDF [58]

Some other methods for the synthesis of PVDF include radiation or plasma induced polymerisation and polymerisation in supercritical CO<sub>2</sub> [58].

## 2.5 PVDF properties

PVDF is a thermoplastic whose properties depend on its molecular weight, molecular weight distribution, crystalline form, chain configurations and the defects of chaining. The interesting properties of PVDF include its piezoelectric, pyroelectrical and ferroelectric behaviour.

PVDF is 50-70% crystalline and exists in 5 crystal polymorphs named  $\alpha$ ,  $\beta$ ,  $\gamma$ ,  $\delta$  and  $\epsilon$ . The most frequent crystal polymorphs are  $\alpha$ ,  $\beta$  and  $\gamma$ . The  $\alpha$  phase is the most thermodynamically stable while the  $\beta$  phase is known for its superior piezoelectric, pyroelectric and ferroelectric properties.

PVDF is inert to most solvents, oils, acids and shows low permeability to gases and liquids. Various properties of PVDF are shown in Table 2.4. The properties in Table 2.4 were obtained by [58].

**Table 2.4:** Properties of PVDF

Property	Value (°C)
Melting temperature	155 to 192
Glass transition temperature	-40 to -30

## 2.6 Copolymerisation of VDF

Copolymerisation is the most general way to modify the properties of polymers and results in a change of the symmetry of the polymer chain. This modification of symmetry results in a change in the intramolecular and intermolecular forces. As a result properties such as melting point, glass transition temperature, crystallinity, elasticity, permeability and chemical resistance can be altered within wide limits [58]. Some well-established copolymers of VDF are poly(VDF-*co*-HFP), poly(VDF-*co*-CTFE), poly(VDF-*co*-TrFE) and poly(VDF-*co*-TFE).

### 2.6.1 Poly(VDF-*co*-HFP) copolymer

Copolymerising VDF with HFP produces random copolymers via emulsion or suspension polymerisation. Since the HFP units cannot homopolymerise in a free radical process no HFP-HFP groups will be found. The presence of the bulky  $\text{CF}_3$  group lowers the degree of crystallinity and the melting temperature while increasing molecular mobility, giving these copolymers better processibility than PVDF [59]. The HFP content influences the type of products that can be formed. For an HFP content less than 15 to 19 mol% the copolymer displays thermoplastic properties and at higher HFP contents the copolymer displays elastomeric behaviour [58]. Copolymers with a 20 to 21 mol% content of HFP display the best compromise between low glass transition temperature and a fully amorphous elastomer.

Crosslinking of the poly(VDF-*co*-HFP) copolymer lead to applications such as gaskets, O-rings, diaphragms for aerospace, automotive or for oil industries [58]. These copolymers have also found use in the energy industry such as membranes for fuel cells, rechargeable lithium ion batteries and dye sensitised solar cells. Poly(VDF-*co*-HFP) copolymer latexes are used in the coating industry and is manufactured by Arkema under the Kynar tradename.

## 2.7 Acrylic modified fluoropolymers

There still remains the challenge to use a PVDF based resin in a low volatile organic compound formulation that performs at comparable levels to solvent based formulations [23]. The chemical inertness of PVDF prevents its adhesion to substrates and makes the dispersion of pigments difficult. Paint formulators add an acrylic modifier resin to overcome these challenges [24]. This acrylic modifier resin can either be physically blended with the PVDF or the surface of the PVDF film can be chemically modified using the methods of graft copolymerisation or core-shell emulsion polymerisation.

## 2.8 Modification of PVDF copolymers

Heterogeneous graft copolymers display properties of both the polymeric backbone as well as the grafts rather than averaging the homopolymer properties. Graft copolymers have properties that are different to those of the homopolymer, the polymer blend and the random copolymers. They also show different properties depending on the composition and the arrangement of the homopolymer sequences [60].

Graft copolymers have been useful for surface modification of polymers and also to improve the miscibility of immiscible homopolymers. According to [60] fluorine-containing graft copolymers find applications in the fields of coatings, adhesives, films, fibres and mouldings due to their miscibility and low surface energy.

Core-shell particles are prepared by a series of emulsion polymerisation steps with different monomers [61]. During the first step, the monomers are polymerised and then used as seed particles in the second stage of polymerisation with other monomers. The initial polymer that is created in the first stage usually forms the inner part [38–42].

These methods are used to impart different functional groups to polymers thereby incorporating specific properties into the material but also maintaining desirable properties of the parent polymer. In poly(VDF-co-HFP) copolymer the active sites able to initiate a polymerisation are the alkyl radicals namely the mid-chain  $-\text{CF}_x-\text{CH}_2-\text{CF}_x$  and end-chain  $-\text{CF}_2-\text{CH}_2-$  [32]. In this way chemical changes to the polymer can result in changes to the wettability, surface tension and adhesion [33].

## 2.9 Commercial PVDF coatings

PVDF has been commercially available since 1961. Elf Atochem (now Arkema) was one of the first companies to commercialise PVDF for coating applications and for melt processing. Some of the coatings sold by Arkema are shown in Table 2.5

**Table 2.5:** Coatings manufactured by Arkema [10]

Trade Name	Polymer resin	Type of coating
Kynar 500	PVDF	Solvent dispersion
Kynar 500 Plus	PVDF	Water or solvent dispersion
Kynar 500 VLD	PVDF	Solvent dispersion
Kynar 500 PC	PVDF	Powder coating
Kynar SL	VDF-TFE	Solvent dispersion or solution
Kynar ADS	VDF-TFE-HFP	Solvent solution

## 2.10 Characterisation methods

### 2.10.1 Rheology

The study of the rheological properties of coatings is important since it influences the application and performance of the coatings [54]. Viscosity, by definition, is the resistance to flow and rheology is the study of viscosity as a function of shear. Viscosity is dependant on the shear rate and stress of the measuring instrument and the temperature at which the measurement is made as shown in Equation 2.1

$$\eta = \frac{\tau}{D} \quad (2.1)$$

Here  $\eta$ ,  $\tau$ , and  $D$  are the viscosity in poise, shear stress in  $\text{dyn.cm}^{-2}$ , and shear rate in  $\text{s}^{-1}$ , respectively. Some of the typical processes that coatings undergo and their respective shear ranges are shown in Table 2.6.

**Table 2.6:** Shear ranges of coating processes

Process	Shear range ( $\text{s}^{-1}$ )
Sagging	$10^{-2} - 10^{-1}$
Levelling	$10^{-2} - 10^{-1}$
Dripping	$10^0 - 10^1$
Flow coating	$10^0 - 10^1$
Pumping	$10^0 - 10^2$
Mixing	$10^1 - 10^2$
Dispersion	$10^2 - 10^5$
Spraying	$10^3 - 10^5$
Roller coating	$10^3 - 10^5$
Brushing	$10^3 - 10^4$

### Emulsion rheology

An emulsion comprises two phases which are normally immiscible. Coatings made from fluoropolymer dispersions or latexes are composed of a fluoropolymer as the dispersed phase and water as the continuous phase, as well as a surfactant/emulsifier which lowers the interfacial tension of the two phases and stabilizes the system to an extent. Macro-emulsions are kinetically and thermodynamically unstable. As a result, the emulsion will revert to the two phases from which it was formed over time.

Emulsions range from low viscosities (Newtonian milk-like liquids), to thicker shear thinning materials, to thick cream-like materials. The commonality with all these emulsions is the microstructure which comprises of a continuous liquid phase and a liquid dispersed phase [62].

The factors that affect the rheology of emulsions are [63]:

- Volume fraction of the disperse phase ( $\phi$ )
- Viscosity of the disperse phase
- Droplet size distribution

Dynamic oscillatory measurements are done where the stress and strain are varied sinusoidally at a frequency  $\omega$  and the resulting stress or strain is compared to the applied values [63]. Since fluoropolymer emulsions are viscoelastic the strain lags behind the stress where the phase lag or phase angle is  $\delta$  ( $0 < \delta < 90^\circ$ ). The amplitude ratio of stress and strain gives the complex modulus  $G^*$  which comprises of a real part  $G'$  and an imaginary part  $G''$  [63] shown in Equation 2.2 and Equation 2.3. The real part  $G'$  is the storage modulus or the elastic modulus. On the other hand the imaginary part  $G''$  is the loss modulus or the viscous modulus.

$$G' = |G^*| \cos(\delta) \quad (2.2)$$

$$G'' = |G^*| \sin(\delta) \quad (2.3)$$

These parameters can be used to understand the various breakdown processes in emulsions like thinning of liquid films and coalescence and can be used to predict the long term stability of emulsions.

### 2.10.2 Surface tension

The interfacial tension of polymer latexes can be determined using a microbalance. A plate, ring, rod or other probe of simple shape is brought into contact with the interface. The 2 main techniques for direct measurement of interfacial tension using a microbalance is the Wilhelmy plate technique and the Du Noüy ring method [64]. The Du Noüy ring method is a detachment technique. This means that the interfacial tension is measured by measuring the force required to separate the ring from contact with the interface [65]. The ring is usually made of platinum or a platinum-iridium alloy. The ring is usually 2-3 cm in radius with the wire radius ranging from 1/30 to 1/60 of the ring. The equation used to calculate the interfacial tension ( $\gamma$ ) is shown in Equation 2.5 [65].

$$p = 4\pi R \quad (2.4)$$

$$\gamma = \frac{F}{p(\cos\theta)} f \quad (2.5)$$

In Equation 2.4  $p$  is the perimeter of the three phase contact line which is equal to twice the circumference of the ring. In Equation Equation 2.5  $F$  is the force required to detach the ring from the interface,  $\theta$  is the contact angle measured for the liquid meniscus

in contact with the ring surface and  $f$  is the correction factor that is applied since an additional volume of water is lifted during the detachment of the ring from the interface.

## Chapter 3

# Characterisation of commercial poly(VDF-*co*-HFP) copolymer

### 3.1 Introduction

Understanding the properties of the base latex is crucial to understanding the behaviour of poly(VDF-*co*-HFP) during emulsion copolymerisation with acrylic monomers.

This chapter documents the characterisation of the commercial poly(VDF-*co*-HFP) fluoropolymer latex. Methods of analysis include spectroscopy (ATR-FTIR and  $^{19}\text{F}$  NMR), particle size distribution, rheology, DSC analysis, light microscopy, film formation, solubility, density and surface tension.

### 3.2 Experimental

#### 3.2.1 Materials

Poly(VDF-*co*-HFP) copolymer (solid content 46%) was purchased from Arkema Inc. and used as received. The poly(VDF-*co*-HFP) copolymer was obtained as a aqueous emulsion and stored at ambient conditions.

Dimethyl sulfoxide (DMSO), deuterated d6-DMSO, dimethylformamide (DMF), tetrahydrofuran (THF), pentane, and acetone were purchased from Sigma Aldrich and used as received. The surfactant mixture for particle size analysis was purchased from Unilever.

De-mineralised water was obtained from a Thermoscientific Barnstead Easypure 2 (18M $\Omega$  · cm) that was fed distilled water from an in-house distillation unit. The N<sub>2</sub> (5N) and Ar (5N) were supplied by African Oxygen Ltd.

### 3.2.2 Methods

#### Nuclear magnetic resonance (NMR) spectroscopy

$^{19}\text{F}$  NMR spectroscopy was performed on the commercial poly(VDF-*co*-HFP) copolymer. The NMR spectra were collected using a Bruker Avance III NMR spectrometer equipped with a 5 mm BBO probe. The instrument parameters were a flip angle of  $30^\circ$ , acquisition time 0.7 s, pulse delay 2 s, number of scans 128, pulse width of  $5\ \mu\text{s}$  and spectrometer frequency 376.5 MHz. Deuterated  $\text{d}_6$ -DMSO was used as solvent.

#### Fourier-transform infra-red (FTIR) spectroscopy

The commercial poly(VDF-*co*-HFP) copolymer analysed by attenuated total reflectance (ATR) FTIR using a Perkin-Elmer Spectrum 100 FTIR spectrometer. Samples were scanned from  $600$  to  $4000\ \text{cm}^{-1}$  with an accuracy of  $2\ \text{cm}^{-1}$ .

#### Differential scanning calorimetry (DSC)

The commercial poly(VDF-*co*-HFP) copolymer latex was characterised using DSC using a Mettler-Toledo DSC 1. The samples were encapsulated in aluminium pans with holes punched into the lids. The samples were loaded into the DSC at ambient temperature and then cooled to  $-60\ ^\circ\text{C}$  at a cooling rate of  $10\ ^\circ\text{C} \cdot \text{min}^{-1}$ . The sample was then kept at  $-60\ ^\circ\text{C}$  for 5 min and thereafter heated to  $200\ ^\circ\text{C}$  at a heating rate of  $10\ ^\circ\text{C} \cdot \text{min}^{-1}$ . The samples were run under an  $\text{N}_2$  atmosphere flowing at  $20\ \text{ml} \cdot \text{min}^{-1}$ .

#### Particle size distribution (PSD)

The average particle sizes and the particle size distributions of the commercial poly(VDF-*co*-HFP) copolymer were measured using a Malvern Mastersizer 3000. The Mastersizer uses the method of laser light scattering (Mie scattering) with a 4 mW He-Ne laser light source operating at 632.8 nm. Water was employed as the carrying medium with 1 % by weight of a surfactant mixture (Sodium dodecylbenzene sulfonate, sodium lauryl ether sulfate, sodium lauryl ether sulfate, and cocamidopropyl betaine) as dispersant. The measurements were carried out at an obscuration of 10 %. Each sample was analysed 8 times and the results averaged for the final particle size distribution.

### 3.2.3 Light microscopy

The commercial poly(VDF-*co*-HFP) copolymer was viewed under a light microscope (Nikon Corporation, Japan) and images were recorded.

## Viscosity

The viscosities of the latexes were measured using a Brookfield DVIII Ultra Programmable Rheometer. The Rheometer was operated at 10 rpm and 25 °C. Temperature control was effected by way of a Ghant heat transfer bath.

## Density and surface tension

The density and surface tension of the commercial poly(VDF-*co*-HFP) copolymer were determined using an Attension Sigma 700 force tensiometer. The surface tension was assessed using the du Noüy ring method [66]. The density was determined using a density probe with known mass and volume.

## Solubility

Solubility tests were conducted on the dried films of the poly(VDF-*co*-HFP) copolymer. DMF, THF, acetone and DMSO were employed as solvents. Samples of the polymers were placed in test tubes with a set amount of solvent added. The tubes were vortexed and solubility was determined qualitatively by observing if any solid material appeared to have dissolved.

## Adhesion and peel test

Adhesion testing was conducted according to the ASTM D3359-09 standard [75]. The test method used is similar to that used for assessing adhesion on a metallic substrates by applying and removing pressure sensitive tape over cuts made in the film.

2 mL of the poly(VDF-*co*-HFP) copolymer latex was placed on the surface of clean, dry, flat, glass plates, and spread out to cover an area of 900 mm<sup>2</sup>. The glass plates were degreased beforehand *via* sequential washing with pentane, ethanol, and water. The latex was air dried at ambient temperature (23 °C) for 65 min to form an even film. The remaining solvent (water) was then evaporated in a oven at 120 °C for 10 min. The dry film was then left to cool to ambient temperature before the adhesion test was conducted. The adhered film was cut into a grid pattern. Each grid square was 20 mm long and the squares were spaced 2 mm apart. The film between the squares was carefully peeled from the glass plate with a scalpel. Broad adhesive tape was then placed over the grid and smoothed out. Removal of the tape occurred within 90 s of application. Removal was effected by hand.

## Film formation

A sample of the poly(VDF-*co*-HFP) copolymer latex was deposited in clean glass Petri dish and dried in an oven at 80 °C for 16 hours. The Petri dish were degreased beforehand

*via* sequential washing with pentane, ethanol, and water. The films were rated in arbitrary categories according to their appearance. The film formation experiments were repeated at 25 °C and 50 °C to verify the reported minimum film-forming temperatures.

### 3.2.4 Rheology

Dynamic oscillatory measurements were also carried out on the poly(VDF-*co*-HFP) copolymer latex using a rheometer (Physica MCR301, Anton Paar, UK) with a plate and plate geometry. A strain is applied sinusoidally with a frequency  $\omega$  ( $\text{rad} \cdot \text{s}^{-1}$ ) and an amplitude  $\gamma_0$ . This is achieved by moving one of the plates back and forth in a sinusoidal manner and the stress and stress amplitude ( $\sigma_0$ ) on the other plate is simultaneously measured. The complex modulus ( $G^*$ ) is then determined from the ratio of the stress amplitude and the strain amplitude as shown in Equation 3.1. The loss modulus ( $G''$ ), the storage modulus ( $G'$ ) and the damping factor ( $\tan \delta$ ) are determined using Equation 3.2, Equation 3.3 and Equation 3.4 [67].

$$|G^*| = \frac{\sigma_0}{\gamma_0} \quad (3.1)$$

$$G' = |G^*| \cos \delta \quad (3.2)$$

$$G'' = |G^*| \sin \delta \quad (3.3)$$

$$\tan(\delta) = \frac{G''}{G'} \quad (3.4)$$

The storage modulus, loss modulus and damping factor of the poly(VDF-*co*-HFP) copolymer latex was measured at 20 °C, 30 °C, 50 °C and 70 °C.

## 3.3 Results and discussion

The FTIR spectra of the poly(VDF-*co*-HFP) copolymer are presented in Figure 3.1. The micrographs at 100X magnification of the poly(VDF-*co*-HFP) copolymer are presented in Figure 3.2. The particle size distribution is shown in Figure 3.3 and is the average of 8 measurements. The viscosity results are shown in Figure 3.4. The resultant heat flow versus temperature curve from DSC analysis is shown in Figure 3.5. The moduli obtained from rheological measurement is shown in Figure 3.6. The  $^{19}\text{F}$  NMR spectrum for the poly(VDF-*co*-HFP) copolymer is shown in Figure 3.7. The tensiometry results are shown in Table 3.1.

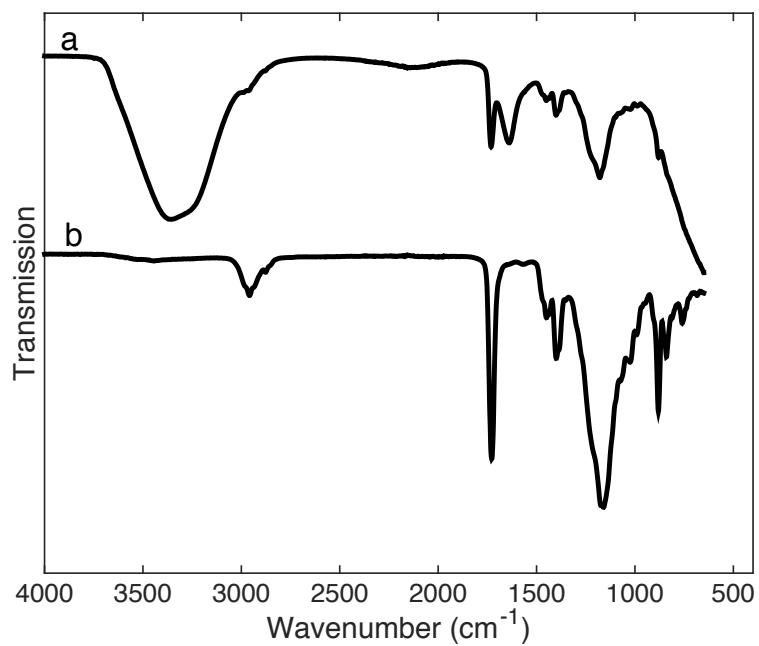


**Figure 3.1:** ATR-FTIR spectra of poly(VDF-*co*-HFP) copolymer latex and film

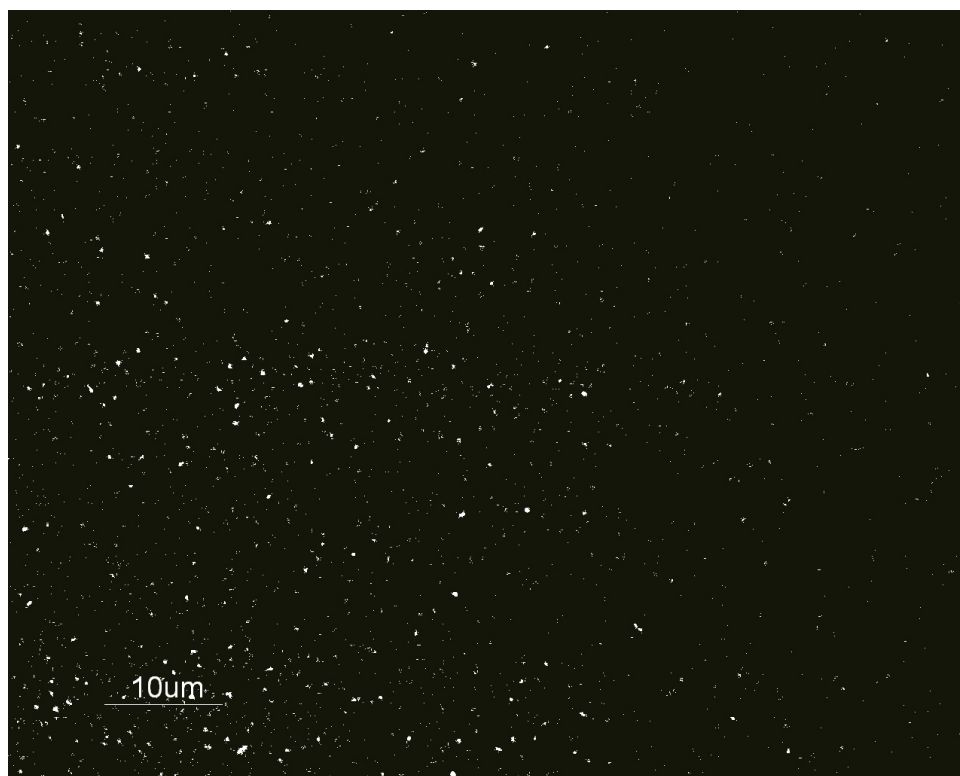


**Figure 3.2:** Microscopic photograph of poly(VDF-*co*-HFP) copolymer appearing as white dots

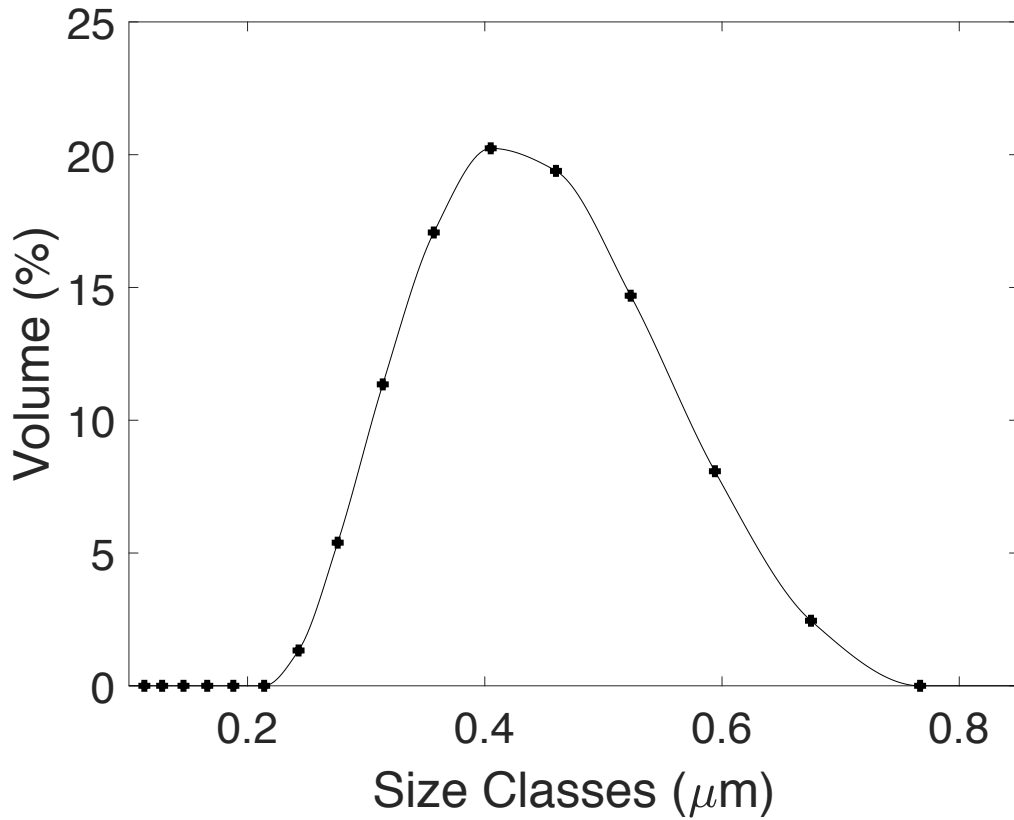


**Figure 3.3:** Particle size distribution of poly(VDF-*co*-HFP) copolymer

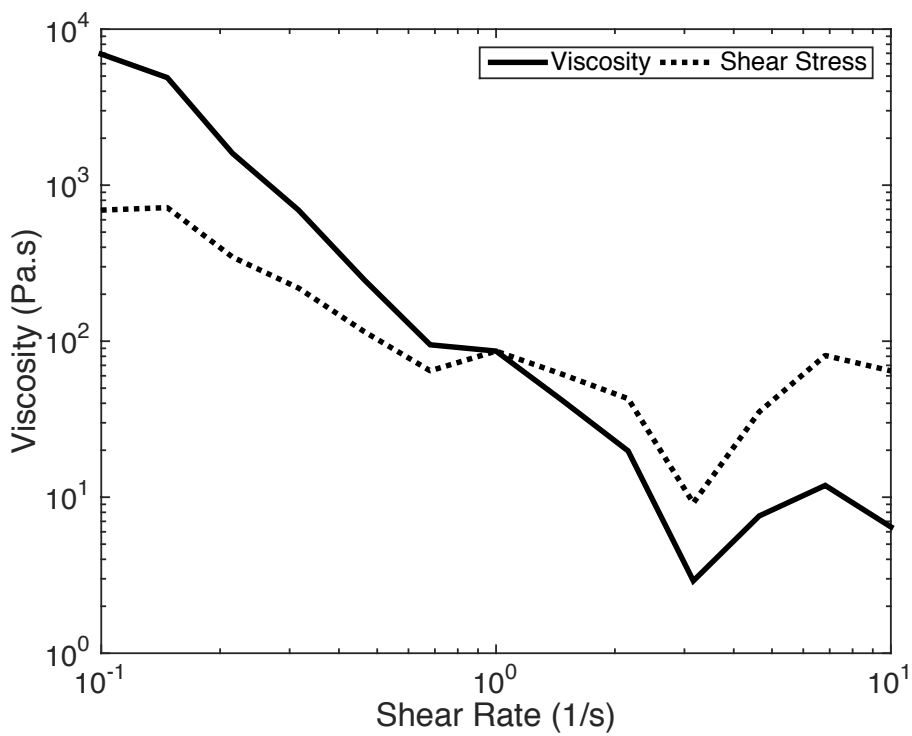


**Figure 3.4:** Viscosity of poly(VDF-*co*-HFP) copolymer

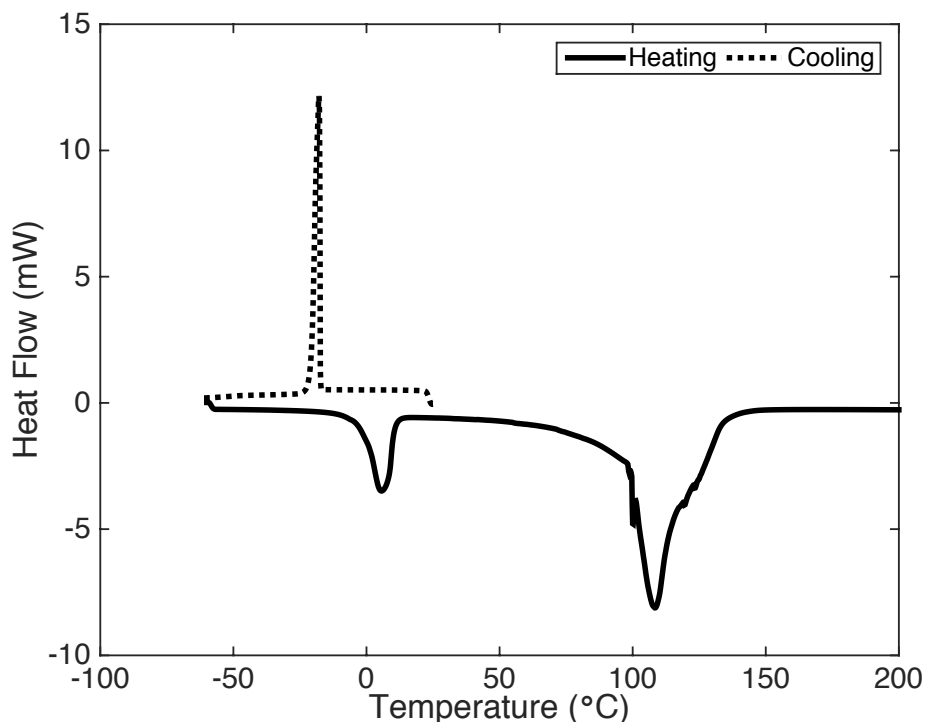


**Figure 3.5:** DSC curve of poly(VDF-*co*-HFP) copolymer

**Table 3.1:** Density and surface tension results

Latex	Density ( $\text{g} \cdot \text{cm}^{-3}$ )	Surface tension ( $\text{mN} \cdot \text{m}^{-1}$ )
poly(VDF- <i>co</i> -HFP) copolymer	1.14	32.47

### 3.3.1 Structure and composition of the polymers

The distinctive band at  $3325 \text{ cm}^{-1}$  is assigned to the OH stretching from the water in the latexes. The band at  $1181 \text{ cm}^{-1}$  is attributed to CF stretching. Additional absorbance bands are observed in the FTIR spectra of the films. The band at  $2959 \text{ cm}^{-1}$  is attributed to the CH stretching vibration. The microstructure of VDF-based copolymers can be resolved by  $^{19}\text{F}$  NMR.

Figure 3.7 displays the  $^{19}\text{F}$  NMR spectrum of the poly(VDF-*co*-HFP) copolymer. The signals related to HFP units are:  $\text{CH}_2\text{-CF}_2\text{-CF}(\text{CF}_3)\text{-CF}_2$ , at 70.18 ppm,  $\text{CF}_2\text{-CF}(\text{CF}_3)\text{-CH}_2\text{-CF}_2\text{-}$  at -74.59 ppm and  $\text{CH}_2\text{-CF}_2\text{-CF}_2\text{-CF}(\text{CF}_3)\text{-CH}_2\text{-CF}_2\text{-CF}_2\text{-CF}(\text{CF}_3)$  at -75.0 ppm correspond to the fluorine nuclei of the  $\text{CF}_3$  group; signals  $\text{CH}_2\text{-CF}_2\text{-CF}(\text{CF}_3)\text{-}$  at -103.45 ppm and  $\text{-CF}_2\text{-CF}_2\text{-CF}(\text{CF}_3)\text{-}$  at -118.56 ppm to  $\text{CF}_2$  and  $\text{CF}_2\text{-CF}(\text{CF}_3)\text{-CF}_2\text{-}$  at -182.3 ppm,  $\text{CF}_2\text{-CF}(\text{CF}_3)\text{-CH}_2\text{-}$  at -185.0 ppm and  $\text{CF}_2\text{-CF}(\text{CF}_3)\text{-CH}_2\text{-CF}_2\text{-CF}_2\text{-CF}(\text{CF}_3)$  at -185.2 ppm to the CF group of the HFP repeating unit, respectively [68]. The  $^{19}\text{F}$  NMR spectrum exhibits also various groups of signals assigned to VDF units and are

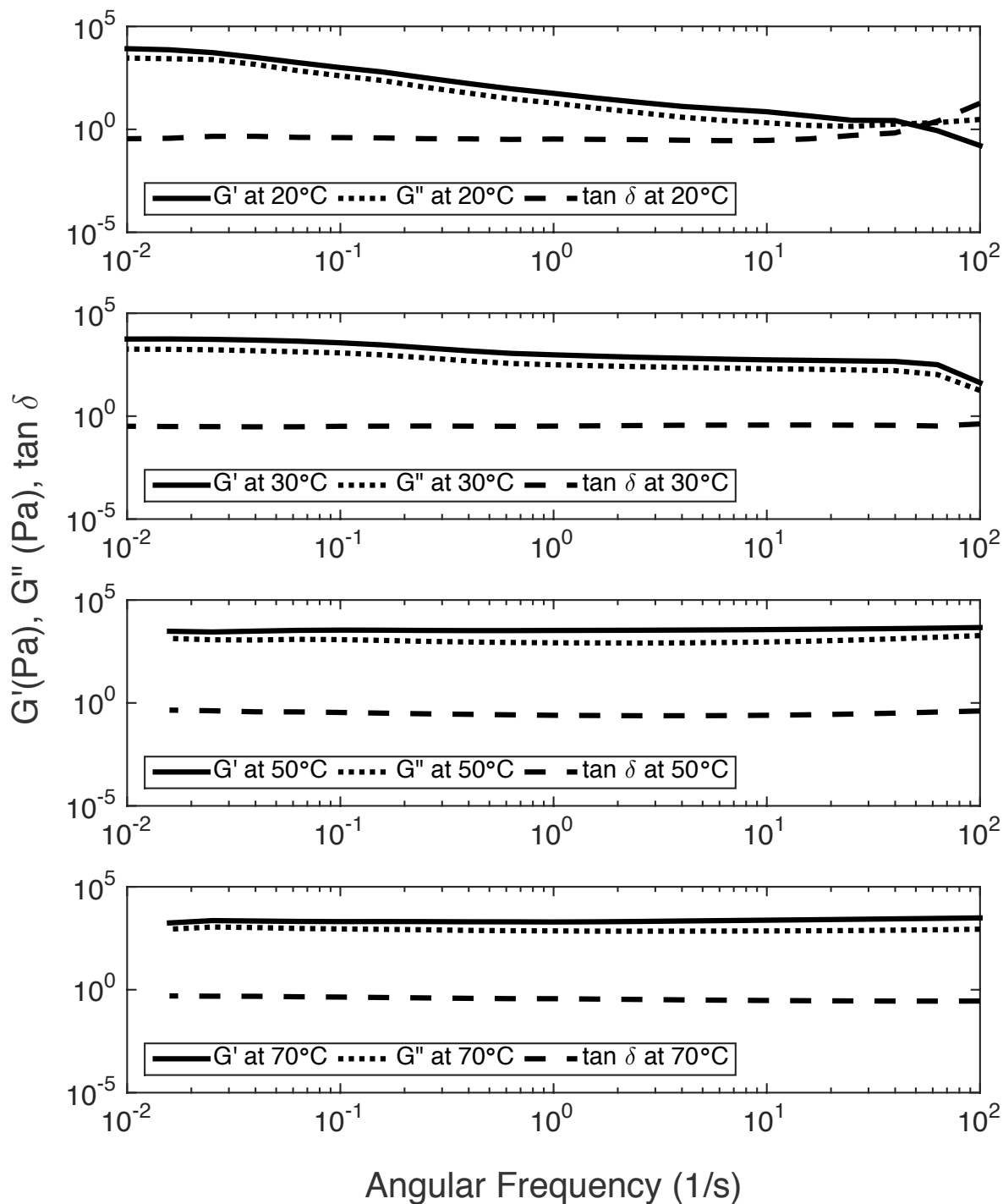


**Figure 3.6:** Storage modulus ( $G'$ ), loss modulus ( $G''$ ) and damping factor ( $\tan \delta$ ) measured as a function of angular frequency at 20 °C, 30 °C, 50 °C and 70 °C

centred at -91.9 to -96.73 ppm for head-to-tail normal additions ( $-\text{CH}_2\text{CF}_2-\text{CH}_2\text{CF}_2-$ ), at -108.75 to -112.47 ppm for  $\text{CF}_2$  groups adjacent to a HFP unit ( $-\text{CH}_2\text{CF}_2\text{CF}_2\text{CF}(\text{CF}_3)-$ ), and at -113.6 and -116.1 ppm for the head-to-head reversed addition ( $-\text{CH}_2\text{CF}_2-\text{CF}_2\text{CH}_2-$ ) of VDF [69].

The VDF mol percentage can be obtained from Equation 4.1 [70, 71], where [VDF] is the mol percentage of VDF in the copolymer,  $\int \text{CF}_2$  is the integration of the peaks c to

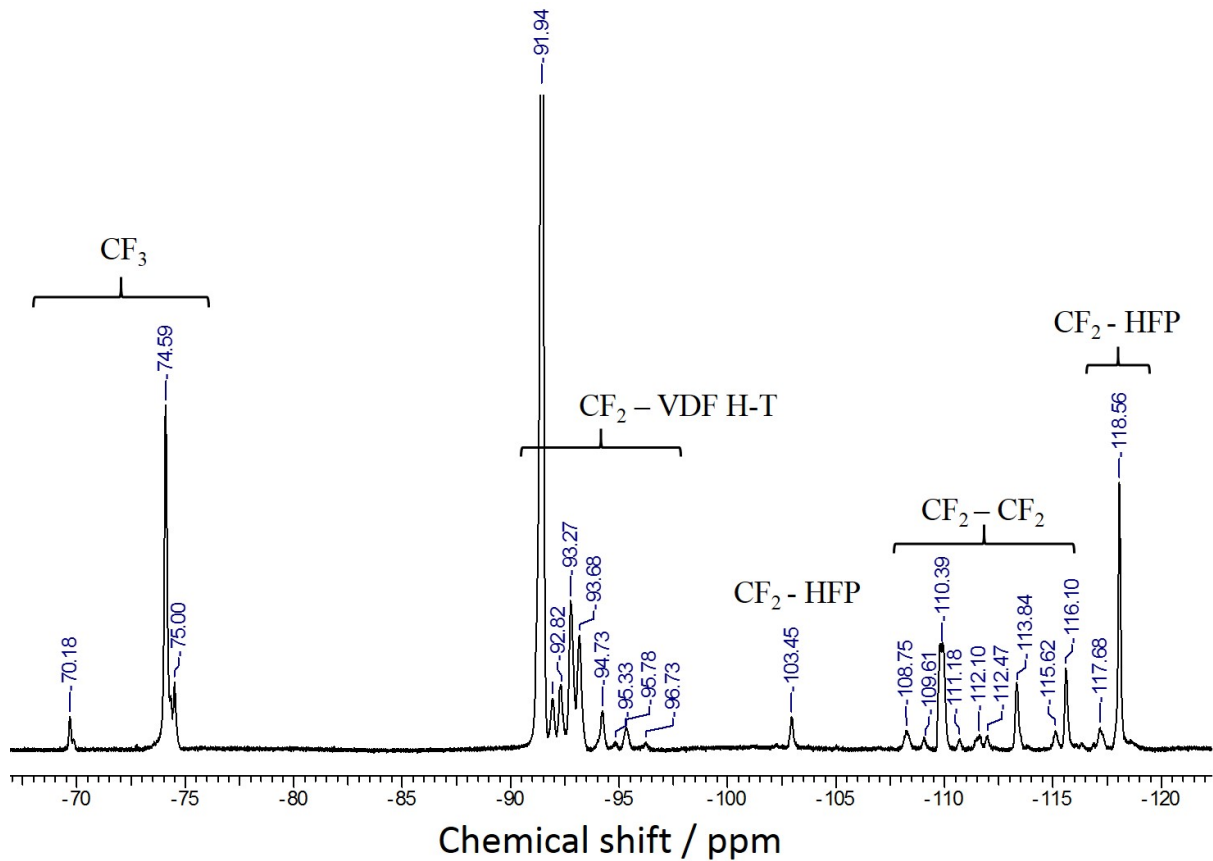


**Figure 3.7:** Experimental  $^{19}\text{F}$  NMR spectrum of poly(VDF-*co*-HFP) copolymer

$k$  and  $\int \text{CF}_3$  is the integration of peaks a and b.

$$[\text{VDF}] = \frac{\int_{-90}^{-117} \text{CF}_2/2}{\int_{-90}^{-117} \text{CF}_2/2 + \int_{-70}^{-75} \text{CF}_3/3} \quad (3.5)$$

Using Equation 4.1 and integrating under the peaks as in Figure 3.7 the mol percentage of VDF was calculated as 87.9% and the mol percentage of HFP was 12.1%.

### 3.3.2 Particle size and morphology

The average particle size of the poly(VDF-*co*-HFP) copolymer latex was found to be approximately 0.41  $\mu\text{m}$ . The particle size distribution of the latex was unimodal as shown in Figure 3.3. According to [47] the latex may be classified in the medium range (0.3  $\mu\text{m}$  to 2  $\mu\text{m}$ ). For unimodal particle size distributions the maximum packing factor for random distributions is 0.64 [47].

Under light microscopy, the latex particles appear brighter than the background as shown in Figure 3.2 this is due to the size of the particles being smaller than the wavelength of light used [72].

### 3.3.3 Flow properties

The viscosity results (Figure 3.4) indicate that the poly(VDF-*co*-HFP) copolymer behaves as a non-Newtonian fluid since the viscosity decreases with increasing shear rate. Specifically, the poly(VDF-*co*-HFP) copolymer is shear thinning.

Since the storage modulus ( $G'$ ) is a measure of the energy stored in a cycle of oscillation a decreasing  $G'$  would indicate an unstable latex. A flat profile of the storage modulus ( $G'$ ) against angular frequency (Figure 3.6) is measured at 20 °C, 30 °C, 50 °C and 70 °C. At 20 °C and 30 °C the storage modulus increases with a decrease of angular frequency. This is attributed to the poly(VDF-*co*-HFP) copolymer forming a film in the rheometer at these temperatures which is due to the evaporation of some of the water shown in Figure 3.8.

$\tan \delta$  is approximately 1 (Figure 3.6) for all temperatures measured, which indicates that the latex has equal elastic and viscous components.

The surface tension affects the emulsion wetting on substrates and a lower surface tension would result in better flow property as well as adhesion to substrates [73]. The density of the poly(VDF-*co*-HFP) copolymer latex was found to be  $1.14 \text{ g} \cdot \text{cm}^{-3}$  and the surface tension was  $32.47 \text{ mN} \cdot \text{m}^{-1}$ .



**Figure 3.8:** Photograph of poly(VDF-*co*-HFP) copolymer latex after rheology tests

The differential scanning calorimetry cooling curve (Figure 3.5) shows a crystallisation peak at  $-12.97 \text{ }^\circ\text{C}$ . On the heating curve the peak at  $7.03 \text{ }^\circ\text{C}$  is attributed to the melting of the sample. Three overlapping melting peaks are observed at  $108 \text{ }^\circ\text{C}$ . One explanation for this is the boiling of the water and volatiles and two crystalline regions of the poly(VDF-*co*-HFP) copolymer. The higher melting peak is the more organised crystalline region than the other which may be the anchored amorphous phase [74]. No visible  $T_g$  is observed from the DSC curve.

## 3.4 Conclusions

The structure of the poly(VDF-*co*-HFP) copolymer is composed of a VDF-HFP backbone with 87.9 % VDF and 12.1 % HFP (assuming only VDF and HFP in the latex) determined via  $^{19}\text{F}$  NMR spectroscopy.

When comparing the ATR-FTIR spectrum of the latex to the dry film, the proposed mechanism of film formation is: the evaporation of the water from the latex.

The work done by [24] describes the production of the aqueous fluoropolymer produced by Arkema. This is a 2 step polymerisation using the poly(VDF-*co*-HFP) copolymer as a seed particle, therefore the proposed morphology of the latex particles is a core-shell structure. This morphology needs to be confirmed with SEM.

The average particle size of the latex was determined to be  $0.41\ \mu\text{m}$  with a unimodal particle size distribution. The particle sizes are smaller than the wavelength of light used in light microscopy. This causes the particles to appear bright against a dark background when viewed under a light microscope.

The flow properties of the latex were determined using a rheometer. The latex was found to be shear thinning and the storage modulus was constant with changing angular frequency at  $50\ ^\circ\text{C}$  and  $70\ ^\circ\text{C}$ . At  $20\ ^\circ\text{C}$  and  $30\ ^\circ\text{C}$  the latex started to dry in the rheometer resulting in an increased storage modulus at decreasing angular frequency.

The DSC analysis of the latex showed a crystallisation peak at  $-12.87\ ^\circ\text{C}$  and a melting peak at  $7.03\ ^\circ\text{C}$ . Three overlapping melting peaks were observed at  $108\ ^\circ\text{C}$  which are attributed to the boiling off of the water and the volatiles in the latex and the 2 crystalline regions of the poly(VDF-*co*-HFP) copolymer.

The surface tension and density of the latex was also determined using a tensiometer. The surface tension was  $32.17\ \text{mN} \cdot \text{m}^{-1}$  and the density was  $1.14\ \text{g} \cdot \text{cm}^{-3}$ .

# Chapter 4

## Modification of poly(VDF-*co*-HFP) copolymer

### 4.1 Introduction

This chapter documents the modification of the commercial poly(VDF-*co*-HFP) copolymer based on the work by Kato *et al.* [49]. The method of modification is core-shell emulsion polymerisation with a mixture of monomers. The experimental setup and core-shell emulsion polymerisation is described and the products of these reactions are then characterised and compared to the unmodified commercial latex.

### 4.2 Experimental

#### 4.2.1 Materials

Poly(VDF-*co*-HFP) copolymer (solid content 46%) was purchased from Arkema Inc. and used as received. The poly(VDF-*co*-HFP) was obtained as a aqueous emulsion and stored at ambient conditions.

Methyl methacrylate (MMA), methacrylic acid (MA), styrene (S), n-butyl acrylate (NBA), ethyl acrylate (EBA), acrylic acid (AA), sodium dodecyl sulfate (SDS) and sodium persulfate (SPS) were purchased from Merck and used as received. The monomers were stored at *ca* 4°C until used. Dimethyl sulfoxide (DMSO), deuterated d6-DMSO, dimethylformamide (DMF), tetrahydrofuran (THF), pentane, and acetone were purchased from Sigma Aldrich and used as received. The surfactant mixture for particle size analysis was purchased from Unilever.

De-mineralised water was obtained from a Thermoscientific Barnstead Easypure 2 (18M $\Omega$  · cm) that was fed distilled water from an in-house distillation unit. The N<sub>2</sub> (5N) and Ar (5N) were supplied by African Oxygen Ltd.

## 4.2.2 Methods

### Emulsion polymerisation

The materials and their weight percentages were based on Kato *et al.*[49]. MMA, MA, S, NBA, EA and AA were used as monomers. SDS was used as surfactant and SPS was used as the radical initiator. An emulsion mixture was made with the monomers, 25 mL water and 0.1 g of sodium dodecyl sulfate as the surfactant. This mixture was obtained by emulsion mixing the components at 5000 rpm for 10 min using a Silverson High Shear Mixer. The composition of monomer emulsion mixtures used in the formation of each latex are shown in Table 4.1. The reaction was carried out in a 1 L round bottom flask equipped with a stirrer and thermometer. 50 mL poly(VDF-*co*-HFP) copolymer, 75 mL water and 0.15 g sodium persulfate were added to the flask, degassed with argon for 10 min and then sealed with a rubber septum. The flask was then heated in a water bath to 75 °C and stirred for 15 min. The monomer mixture was fed into the round bottom flask using a syringe and needle over a period of 2 h while stirring was kept constant at 200 rpm. The monomer mixture was added drop wise to the flask with an average drop volume of 3 mL for latexes 1 to 4 and 21 mL for latexes 5 to 8. The mixture was left to react 30 min after all the monomer emulsion was added. No further purification of the latexes was carried out after the reaction. The product latexes were stored at ambient conditions (*ca* 25 °C) before being subjected to analysis.

Latexes 5 to 8 use the same combination and weight ratios of monomers as latexes 1 to 4, however the total volume of the monomer was increased by a factor of 7 as shown in Table 4.1.

**Table 4.1:** Variation of monomers in volume (ml) for latexes 1 to 8

Monomer	Latex							
	1 (ml)	2 (ml)	3 (ml)	4 (ml)	5 (ml)	6 (ml)	7 (ml)	8 (ml)
n-Butyl acrylate	1.2	-	1.9	-	8.5	-	14.16	-
Methyl methacrylate	1.7	3	-	1.5	12	21	-	10.6
Methacrylic acid	0.13	-	-	-	1	-	-	-
Acrylic acid	-	-	-	0.13	-	-	-	0.95
Styrene	-	-	1.1	-	-	-	8.25	-
Ethyl acrylate	-	-	-	1.4	-	-	-	9.7

### NMR spectroscopy

<sup>19</sup> NMR spectroscopy was performed on films made from latexes 5 to 8. The NMR spectra were collected using a Bruker Avance III NMR spectrometer equipped with a

5 mm BBO probe. The instrument parameters were a flip angle of  $30^\circ$ , acquisition time 0.7 s, pulse delay 2 s number of scans 128, a pulse width of  $5 \mu\text{s}$  and spectrometer frequency 376.5 MHz. Deuterated  $d_6$ -DMSO was used as solvent.

### **FTIR spectroscopy**

Latexes 1 to 8 were analysed by attenuated total reflectance (ATR) FTIR using a Perkin-Elmer Spectrum 100 FTIR spectrometer. Samples were scanned from 600 to  $4000 \text{ cm}^{-1}$  with an accuracy of  $2 \text{ cm}^{-1}$ .

### **DSC**

Latexes 5 to 8 and the poly(VDF-*co*-HFP) copolymer latex was characterised using DSC using a Mettler-Toledo DSC 1. The samples were encapsulated in aluminium pans with holes punched into the lids. The samples were loaded into the DSC at ambient temperature and then cooled to  $-60^\circ\text{C}$  at a cooling rate of  $10^\circ\text{C} \cdot \text{min}^{-1}$ . The sample was then kept at  $-60^\circ\text{C}$  for 5 min and thereafter heated to  $200^\circ\text{C}$  at a heating rate of  $10^\circ\text{C} \cdot \text{min}^{-1}$ . The samples were run under and  $\text{N}_2$  atmosphere flowing at  $20 \text{ ml} \cdot \text{min}^{-1}$ .

### **PSD**

The average particle sizes and the particle size distributions of latexes 1 to 8 were measured using a Malvern Mastersizer 3000. The Mastersizer uses the method of laser light scattering (Mie scattering) with a 4 mW He–Ne laser light source operating at 632.8 nm. Water was employed as the carrying medium with 1 % by weight of a surfactant mixture (Sodium dodecylbenzene sulfonate, sodium lauryl ether sulfate, sodium lauryl ether sulfate, and cocamidopropyl betaine) as dispersant. The measurements were carried out at an obscuration of 10 %. Each sample was analysed 8 times and the results averaged for the final particle size distribution.

### **Viscosity**

The viscosities of the latexes were measured using a Brookfield DVIII Ultra Programmable Rheometer. The Rheometer was operated at 10 rpm and  $25^\circ\text{C}$ . Temperature control was effected by way of a Ghant heat transfer bath.

### **Density and surface tension**

The density and surface tension of the latexes 5 to 8 were determined using an Attension Sigma 700 force tensiometer. The surface tension was assessed using the du Noüy ring method [66]. The density was determined using a density probe with known mass and volume.

## Solubility

Solubility tests were conducted on the dried films of latex 5 to 8 and poly(VDF-*co*-HFP) copolymer. DMF, THF, acetone and DMSO were employed as solvents. Samples of the polymers were placed in test tubes with a set amount of solvent added. The tubes were vortexed and solubility was determined qualitatively by observing if any solid material appeared to have dissolved.

## Adhesion and peel test

Adhesion testing was conducted according to the ASTM D3359-09 standard [75]. The test method used is similar to that used for assessing adhesion on a metallic substrates by applying and removing pressure sensitive tape over cuts made in the film.

2 mL of each latex was placed on the surface of clean, dry, flat, glass plates, and spread out to cover an area of 900 mm<sup>2</sup>. The glass plates were degreased beforehand *via* sequential washing with pentane, ethanol, and water. The latexes were air dried at ambient temperature (23 °C) for 65 min to form an even film. The remaining solvent (water) was then evaporated in a oven at 120 °C for 10 min. The dry films were then left to cool to ambient temperature before the adhesion test was conducted. The adhered film was cut into a grid pattern. Each grid square was 20 mm long and the squares were spaced 2 mm apart. The film between the squares was carefully peeled from the glass plate with a scalpel. Broad adhesive tape was then placed over the grid and smoothed out. Removal of the tape occurred within 90 s of application. Removal was effected by hand.

## Film formation

A sample of each latex was deposited in clean glass Petri dish and dried in an oven at 80 °C for 16 hours. The Petri dish were degreased beforehand *via* sequential washing with pentane, ethanol, and water. The films were rated in arbitrary categories according to their appearance. The film formation experiments were repeated at 25 °C and 50 °C to verify the reported minimum film-forming temperatures.

## 4.3 Results and discussion

The eight latexes obtained after polymerisation were all single phase emulsions. The visual appearance of the films is summarised in Table 4.2. Kato *et al.* [49] report minimum film forming temperatures as high as 50 °C. The minimum film forming temperature depends on the comonomers used during copolymerisation, and this temperature decreasing with increasing hydrophobicity of the comonomers. Contrary to what is claimed by Kato *et al.* [49], all latexes exhibited a film forming temperature lower than 25 °C. The dried

latexes swelled in the presence of DMF, THF, acetone and DMSO. The latexes were never fully soluble in these solvents except for the poly(VDF-*co*-HFP) copolymer that was fully soluble in DMSO.

**Table 4.2:** Film appearance

Film	Appearance
poly(VDF- <i>co</i> -HFP) copolymer	Transparent film
1	Transparent film
2	Transparent film
3	Transparent film
4	Transparent film
5	Transparent film
6	Soft powdery film
7	Transparent, very thin film
8	Opaque, yellowish coloured film

### 4.3.1 Particle size distribution, viscosity, density and surface tension

The viscosity results are displayed in Table 4.3. Measurement 3 for latexes 1 to 8 was taken 2 weeks after the latexes were formed. The results for the density and surface tension are shown in Table 4.4.

The average PSD of latexes 2, 3, 4, 5, and 6 were 0.46  $\mu\text{m}$ , 0.46  $\mu\text{m}$ , 0.52  $\mu\text{m}$ , 0.46  $\mu\text{m}$ , and 0.52  $\mu\text{m}$ , respectively. These latexes therefore, have a larger average particle size than the poly(VDF-*co*-HFP) copolymer latex which is 0.41  $\mu\text{m}$ . This is expected irrespective of whether core-shell or graft polymerisation occurred. Since latexes 5 to 8 have an increased monomer concentration over those of latexes 1 to 4, it is expected that latexes 5 to 8 would have a larger average size than latexes 1 to 4 if grafting occurred. It is assumed that there will be little, if any, termination of the graft polymer chains due to proton transfer from the solvent (water) or the comonomers. However, latex 7 (0.41  $\mu\text{m}$ ) and 8 (0.41  $\mu\text{m}$ ), do not show a significant difference in average particle size compared to the poly(VDF-*co*-HFP) copolymer or to latex 3 and 4.

The viscosity of the latexes as a function of shear rate is shown in Table 4.3. All 8 latexes have a lower viscosity than the poly(VDF-*co*-HFP) copolymer, this is due to the experiments being conducted under dilution. It is noted that, as some latexes age, it loses its viscous strength. This is observed in latexes 3, 5 and 6. However, these observations may be due to experimental errors relating to the accuracy of dilution and are not indicative of any occurrence of coalescence.

The surface tension between the latexes and air are shown in Table 4.4. Latexes 1

**Table 4.3:** Viscosity (cP) of latexes 1 to 8

Latex	Measurement 1 (cP)	Measurement 2 (cP)	Measurement 3 (cP)
poly(VDF- <i>co</i> -HFP) copolymer	130	130	130
Latex 1	4	4	4
Latex 2	4	6	4
Latex 3	6	6	4
Latex 4	4	4	4
Latex 5	6	6	4
Latex 6	6	8	4
Latex 7	6	6	6
Latex 8	6	8	8

to 4 did not exhibit surface tensions that deviated from the base poly(VDF-*co*-HFP) copolymer ( $32.5 \text{ mN} \cdot \text{m}^{-1}$ ). The surface tension of the latexes 5 and 6 ( $31 \text{ mN} \cdot \text{m}^{-1}$ ) were lower than that of the poly(VDF-*co*-HFP) copolymer ( $32.5 \text{ mN} \cdot \text{m}^{-1}$ ). Latex 7 ( $35 \text{ mN} \cdot \text{m}^{-1}$ ) displayed a higher surface tension than that of the poly(VDF-*co*-HFP) copolymer while latex 8 ( $32.4 \text{ mN} \cdot \text{m}^{-1}$ ) was approximately the same as the poly(VDF-*co*-HFP) copolymer.

The surface tension affects the emulsion wetting on substrates and a lower surface tension would result in better flow property as well as better adhesion to substrates [73]. The differences between the base poly(VDF-*co*-HFP) copolymer and latexes 1 to 6 and latex 8 are marginal. The increase in surface tension of latex 7 is attributed to the combined hydrophobic effect of the long chain hydrocarbon in n-butyl acrylate and styrene. The  $^1\text{H}$  NMR spectra did not provide a clear picture of the nature of the copolymerisation between n-butyl acrylate, methyl methacrylate and methacrylic acid, but the surface tension data seems to indicate that the more polar monomers are incorporated into the modified latexes more readily than the more hydrophobic monomers.

**Table 4.4:** Density and surface tension results

Latex	Density ( $\text{g} \cdot \text{cm}^3$ )	Surface Tension ( $\text{mN} \cdot \text{m}^{-1}$ )
poly(VDF- <i>co</i> -HFP) copolymer	1.1	32.5
Latex 5	1.0	31.0
Latex 6	1.0	30.9
Latex 7	1.1	34.7
Latex 8	1.1	32.4

The densities of the latexes did not vary significantly from the density of the base poly(VDF-*co*-HFP) copolymer. Latexes 1 to 4 did not exhibit detectable differences

from that of the base poly(VDF-*co*-HFP) copolymer. The densities also followed the trends seen in the viscosity data in that the latexes produced with polar monomers seems to exhibit lower property values from the base copolymer. It is unclear if this data represents meaningful structural differences between the latexes.

### 4.3.2 Structure and composition of the polymers

The ATR-FTIR spectra for both the emulsions and films for experiments 5 to 8 (Table 4.1) are presented in Figure 4.1 and Figure 4.2. The FTIR spectra for the latexes (Figure 4.1) were invariant for all experiments. The distinctive band at  $3325\text{ cm}^{-1}$  is assigned to the OH stretching from the water in the latexes. The band at  $1731\text{ cm}^{-1}$  is assigned to the stretching vibration of the C=O bond and the band at  $1637\text{ cm}^{-1}$  is assigned to presence of C=C bonds. The bands at  $1400\text{ cm}^{-1}$  and  $1456\text{ cm}^{-1}$  are due to the in-plane bending vibrations of the CH bonds in the  $\text{CH}_3$  group. The band at  $1181\text{ cm}^{-1}$  is attributed to CF stretching. The presence of the C=O bond in all latexes indicate that there are acrylic components in the latexes. Furthermore, the presence of the C=C bond indicates that there is unreacted acrylic in the latexes.

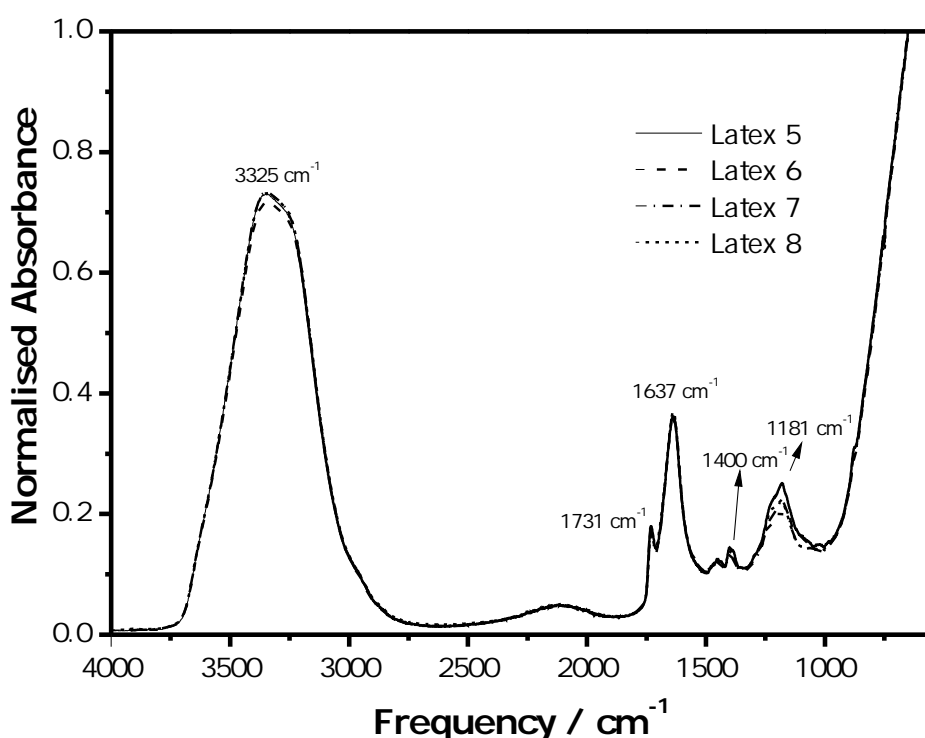


**Figure 4.1:** FTIR spectra of latexes 5 to 8

Additional absorbance bands are observed in the FTIR spectra of the films (Figure 4.2). The band at  $2959\text{ cm}^{-1}$  is attributed to the CH stretching vibration. The

flexing vibration bands of O=C–O–C at 1072 cm<sup>-1</sup> and 1029 cm<sup>-1</sup> are observed in films 5,7 and 8. Film 6 exhibits an increased intensity of the O=C–O–C band at 1051 cm<sup>-1</sup> and 996 cm<sup>-1</sup>. The absorbance band for the C=C bond at 1620 cm<sup>-1</sup> is not observed in the films. This is attributed to the removal of unreacted monomers during the film forming process.

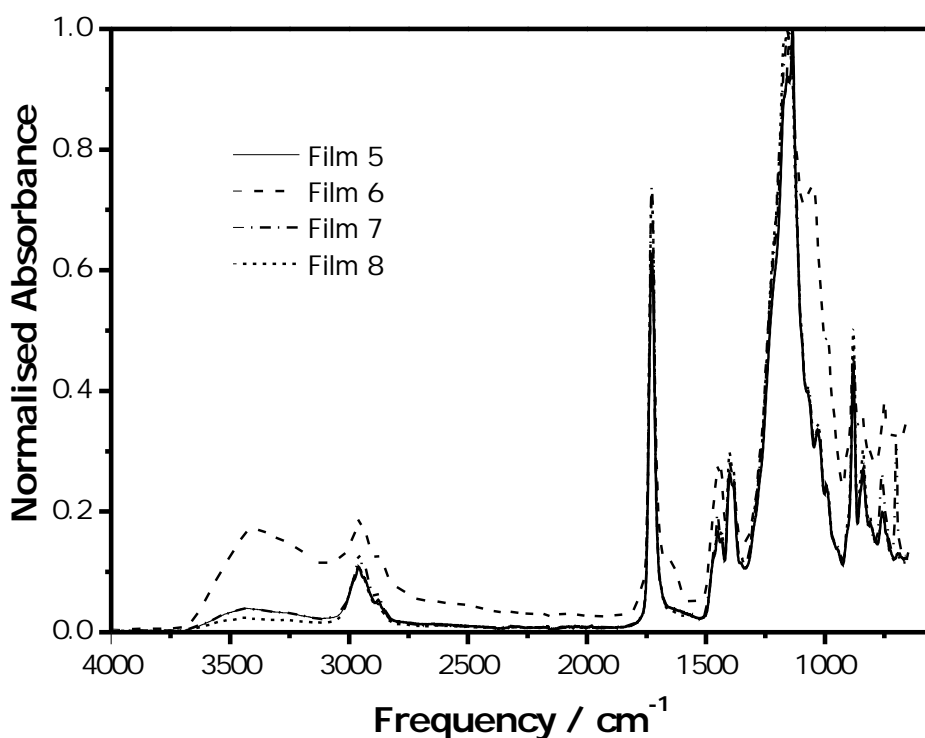


**Figure 4.2:** FTIR spectra of films 5 to 8

The <sup>19</sup>F NMR spectrum for the film of poly(VDF-*co*-HFP) copolymer are presented in Figure 4.3. The structural assignments are according to Pianca *et al.* [71] and Dumas *et al.* [68]. The <sup>19</sup>F NMR spectra for the films of latexes 5, 6, and 7 are shown in Figure 4.4 (the individual spectra are provided in the supporting information). The VDF mol fraction can be obtained from Equation 4.1 [70, 71, 76, 77], where [VDF] is the mol fraction of VDF in the copolymer. The mol fractions of VDF and HFP were calculated as 88 % and 12 %, respectively.

$$[VDF] = \frac{\int_{-90}^{-117} CF_2/2}{\int_{-90}^{-117} CF_2/2 + \int_{-70}^{-75} CF_3/3} \quad (4.1)$$

The product may be either a graft copolymer or a core-shell copolymer. The average bond dissociation energies of the C–H and C–F bonds are 414 kJ · mol<sup>-1</sup> and 485 kJ · mol<sup>-1</sup> for the CH<sub>2</sub> and CF<sub>2</sub>, respectively [78]. Grafting onto perfluorinated polymers is possible, but in the case of PTFE, the grafting process requires generation of an

active site on the polymer chain [79–82]. Therefore, grafting onto the poly(VDF-*co*-HFP) copolymer should occur preferentially at the  $\text{CF}_x\text{-CH}_2\text{-CF}_x$  position.

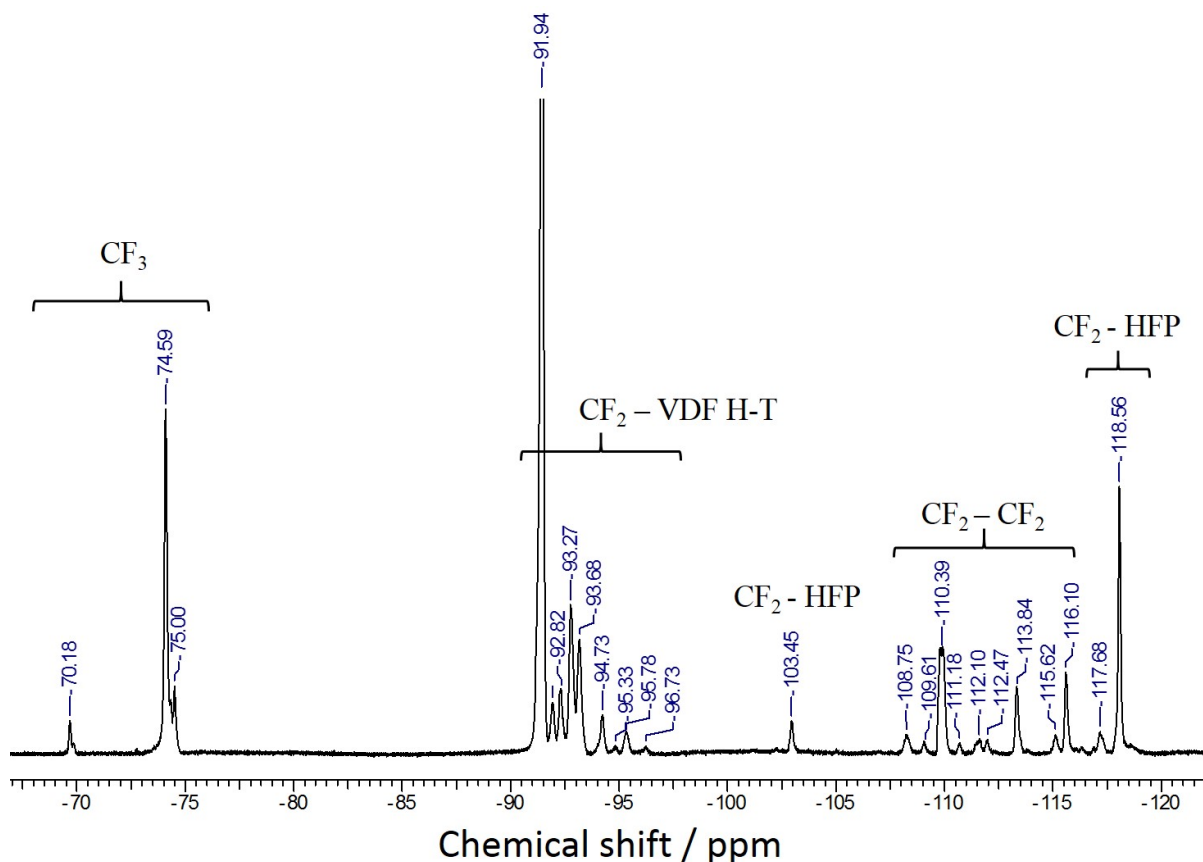


**Figure 4.3:**  $^{19}\text{F}$  NMR spectrum of the unmodified commercial poly(VDF-*co*-HFP) copolymer. The structural assignments are according to Pianca *et al.* [71]

Should grafting occur, the most prominent change should occur in the VDF head-to-tail region (from -90 to -97 ppm). The  $^{19}\text{F}$  NMR spectra of films 5 to 8 are identical to that of the poly(VDF-*co*-HFP) copolymer film which indicates that no modification of the poly(VDF-*co*-HFP) copolymer backbone occurred. The PSD data shows there is a definite increase in the particle size of the modified poly(VDF-*co*-HFP) copolymers over the base copolymer. This shows that the monomers have attached onto the poly(VDF-*co*-HFP) copolymer, but the lack of NMR evidence for grafting seems to indicate that this attachment is mechanical rather than chemical in nature.

Attempts to observe the morphology of the latex emulsion particles by light microscope failed due to a lack of contrast between the presumed acrylic copolymers and the poly(VDF-*co*-HFP) copolymer. Attempts to embed the latex dispersions into a resin and produce sections of the modified poly(VDF-*co*-HFP) copolymer emulsion particles also failed as the polymers seemed to dissolve in the standard resins used for this technique. Therefore, no direct evidence for encapsulation of the poly(VDF-*co*-HFP) copolymer by acrylic copolymers. However, the spectroscopic data strongly indicates that a core-shell

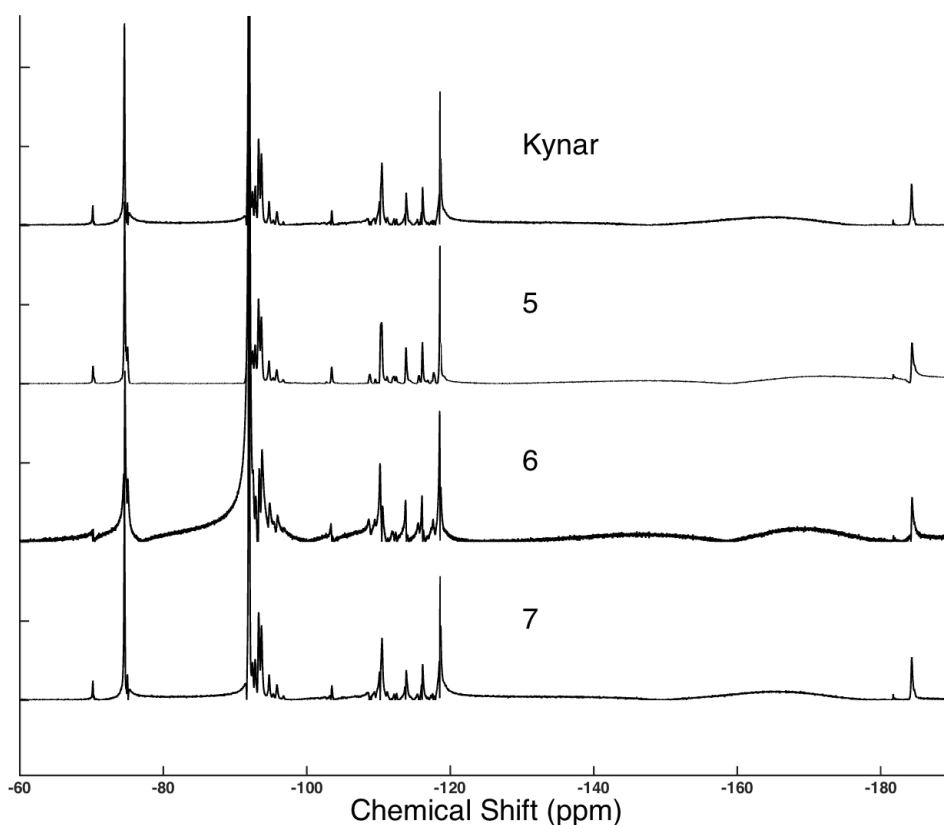


**Figure 4.4:**  $^{19}\text{F}$  NMR spectra of dissolved films 5 to 7 and poly(VDF-*co*-HFP) copolymer

structure is the most likely morphology of the modified poly(VDF-*co*-HFP) copolymer.

### 4.3.3 DSC calorimetry

The heat flow versus temperature plot for the heating curves are shown in Figure 4.5 and the cooling curves are shown in Figure 4.6 for latexes 5, 6, 7, 8, and the base poly(VDF-*co*-HFP) copolymer. The heating curves (Figure 4.5) show a broad melting temperature range at *ca*  $-3^\circ\text{C}$  and three overlapping peaks at  $100^\circ\text{C}$  for both the base- and modified poly(VDF-*co*-HFP) copolymer latexes.

The three peaks at  $100^\circ\text{C}$  can be explained by the evaporation of the water and organic volatiles in the latexes and the melting of the crystalline regions of the poly(VDF-*co*-HFP) copolymer. The higher melting peak is due to the crystalline region and the second highest melting peak may be due to the amorphous region [74]. Latex 6 shows a narrow melting temperature range at  $0.2^\circ\text{C}$ . The latexes also display a shift in the large overlapping peaks compared to the base poly(VDF-*co*-HFP) copolymer. Latexes 6 and 8 show a shift to a lower temperature range of  $97^\circ\text{C}$  and  $96^\circ\text{C}$ , respectively, while latex 5 exhibited a shift to a higher temperature of  $105^\circ\text{C}$ . Latex 7 showed the same overlapping

peaks at 100 °C. Latex 6 also exhibits what appears to be a glass transition at 45 °C.

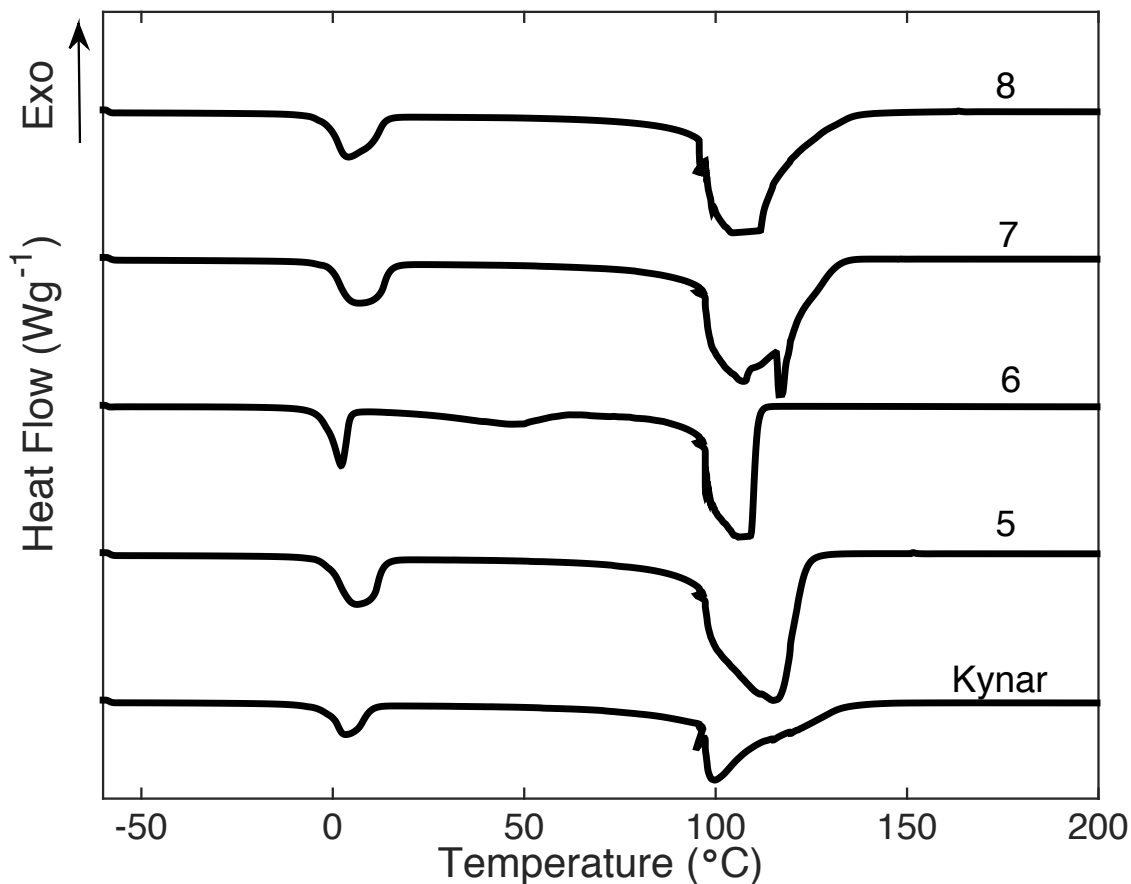


**Figure 4.5:** DSC thermograms of poly(VDF-*co*-HFP) copolymer and latexes 5 to 8 from  $-60^{\circ}\text{C}$  to  $200^{\circ}\text{C}$  at  $10^{\circ}\text{C} \cdot \text{min}^{-1}$

#### 4.3.4 Adhesion and peel test

Results of the peel tests are shown in Table 4.5. The peel test results show that the poly(VDF-*co*-HFP) copolymer displays the strongest adhesion strength, followed by latex 8, the other latexes show weak adhesive properties. For latex 6, no continuous film was formed but rather a powdery residue was observed. Latex 7 exhibited a rubbery texture and when cutting into the latex, the film slipped off the surface. Films peeled cleanly by tape and films that get removed when cutting into squares are considered to have poor to very poor adhesive properties and adhesion tests cannot be conducted on such films [75].

These results directly contradict the claims made by Kato *et al.* [49]. Indeed, the formation of powder over a uniform film for latex 6 seems to support the conclusion that the modified latexes are blends of poly(VDF-*co*-HFP) copolymer and acrylic copolymers. It seems no commercially useful advantage exists for the emulsion copolymerisation of poly(VDF-*co*-HFP) copolymer with acrylic monomers over the solution blending

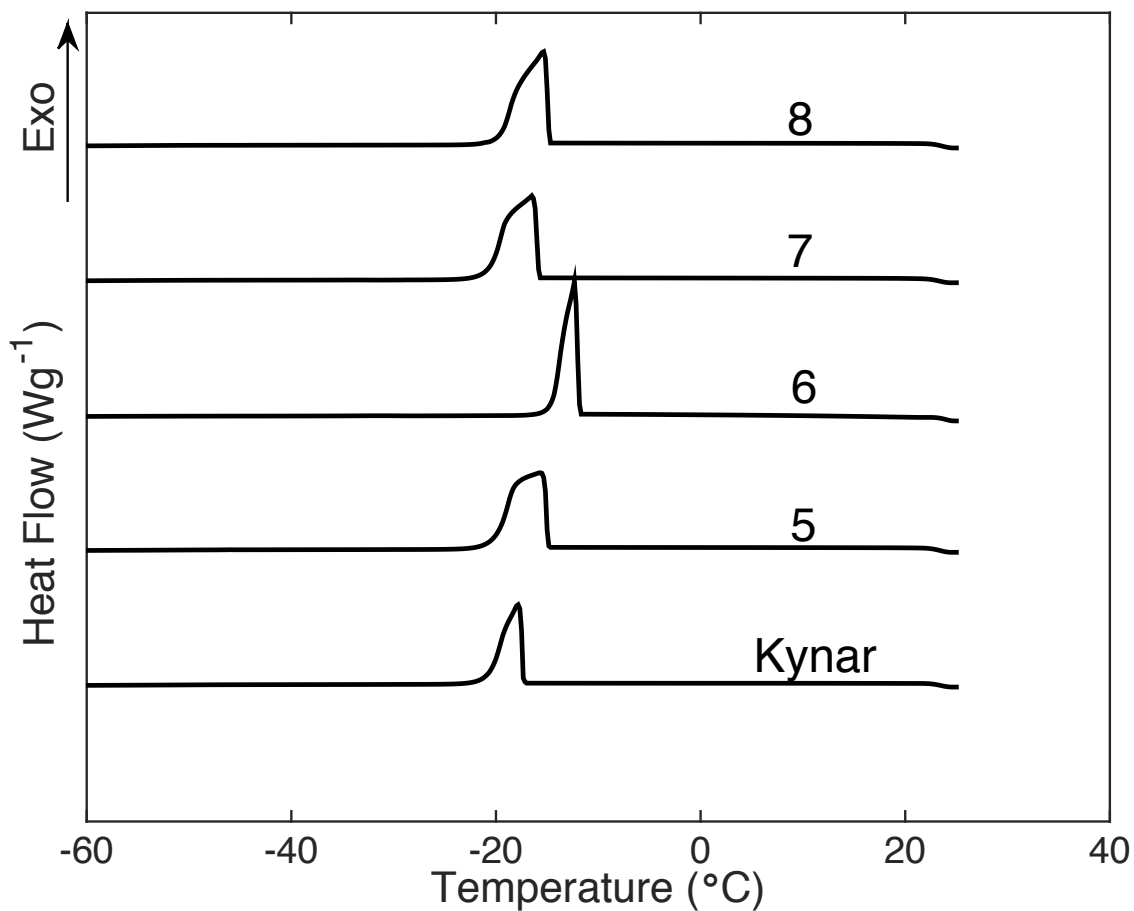


**Figure 4.6:** DSC thermograms of poly(VDF-*co*-HFP) copolymer and latexes 5 to 8 from  $-60\text{ }^{\circ}\text{C}$  to  $25\text{ }^{\circ}\text{C}$  at  $10\text{ }^{\circ}\text{C} \cdot \text{min}^{-1}$

of poly(VDF-*co*-HFP) copolymer with acrylic copolymers as both preparation methods seems to result in the same final product.

**Table 4.5:** Adhesion test results showing the poor quality of the films

Latex	Film area removed (%)
poly(VDF- <i>co</i> -HFP) copolymer	0
Latex 1	75
Latex 2	-
Latex 3	-
Latex 4	-
Latex 5	79
Latex 6	No continuous film formed
Latex 7	Slid off when cutting
Latex 8	22

## 4.4 Challenges

One possible outcome of the reaction could be that the polymer molecule may become too big after the core-shell emulsion polymerisation and would settle out of the latex. Therefore a low initial monomer volume was decided upon to limit the size of the final polymer molecule and this resulted in latexes 1 to 4. Since the polymer molecules did not settle out of the latex, the monomer volume was increased and resulted in the formation of latexes 5 to 8.

In early reactions the dilution of the Kynar was adjusted. When the ratio of total distilled water added to Kynar latex was below 3:2 the latex solidified in the round bottom flask during the experiment as shown in Figure 4.7.



**Figure 4.7:** Solidified latex due to low dilution

## 4.5 Conclusion

The chemical structures of the poly(VDF-*co*-HFP) copolymer and latexes 1 to 8 were characterised using ATR-FTIR and  $^{19}\text{F}$  NMR spectroscopy. ATR-FTIR spectra of the latexes revealed C=O and C=C bonds present in latexes 1 to 8. This indicated that unreacted acrylic components were present. This is expected for latexes 1 to 8 since no removal of the unreacted monomer or any homopolymer was conducted. All films also show the disappearance of the C=C bond as compared to their respective latexes.

The  $^{19}\text{F}$  NMR spectra revealed that the mol fraction of VDF and HFP in the poly(VDF-*co*-HFP) copolymer is 87.9 % and 12.1 %, respectively and that the poly(VDF-*co*-HFP) copolymer backbone was not modified during any of the experiments. This is consistent

with expected results since the active sites available for reaction in poly(VDF-*co*-HFP) copolymer were identified as the mid chain  $\text{CF}_2\text{-CH}_2\text{-CF}_2$  and end chain  $\text{CF}_2\text{-CH}_2$  alkyl radicals.

Latexes 1 to 4 consisted of a low monomer amount in order to prevent precipitation of the poly(VDF-*co*-HFP) copolymer during the experiments. No precipitation was observed during the experiments and the monomer amount was increased by a factor of 7 resulting in latexes 5 to 8. The effect of increased monomer amount was seen in the particle size distributions of the latexes as well as in their viscosities. The average particle size of latexes 2-6 were larger than that of the poly(VDF-*co*-HFP) copolymer indicating that core-shell polymerisation had occurred.

Peel tests demonstrated that no improvement in adhesion properties of the films was observed when modifying the poly(VDF-*co*-HFP) copolymer. The poly(VDF-*co*-HFP) copolymer remained as having the highest adhesion strength, followed by latex 8. This is directly contradictory to the claims made by Kato *et al.* [49].

This study has shown that the physical properties of the commercial poly(VDF-*co*-HFP) copolymer can be modified using the process of core-shell emulsion polymerisation with different acrylic monomers. These properties are melting and crystallisation temperatures, viscosity, surface tension, density and average particle size. However, the claims made in literature [49] could not be substantiated, particularly, the reported improvements in film forming ability was not realised. No commercially useful advantage exists for the emulsion copolymerisation of poly(VDF-*co*-HFP) copolymer with acrylic monomers over the solution blending of poly(VDF-*co*-HFP) copolymer with acrylic copolymers.

Further studies to determine the reaction mechanism and accurate chemical structure need to be done. In particular, determination of the conditions under which grafting will be observed would help in developing better AMF products.

# Chapter 5

## Conclusion

This dissertation proposes a method to reproduce and understand the nature of a poly(VDF-*co*-HFP) based AMF formulation as described by Kato *et al* [49]. Furthermore, claims made by Kato *et al* [49] are investigated and found to be contradictory to experimental results obtained in this work.

### 5.1 Summary of results

#### 5.1.1 Characterisation of commercial poly(VDF-*co*-HFP)

Chapter 3 discussed the characterisation of the commercial poly(VDF-*co*-HFP) to determine benchmark properties. ATR-FTIR confirmed the presence of C=C and C=O bonds in the latex which indicated that unreacted acrylic is present. Comparison of ATR-FTIR results of the dry films and the latex indicated that the film forming mechanism involves the evaporation of water. NMR analysis revealed that the mol fraction of VDF and HFP in the copolymer was 87.9% and 12.1% respectively. Flow characteristics of the commercial poly(VDF-*co*-HFP) was observed to be non-Newtonian and shear thinning. Particle size distribution indicated that the copolymer was unimodal with an average particle size of 0.41  $\mu\text{m}$ . Core-shell morphology of the commercial poly(VDF-*co*-HFP) is proposed since production by Arkema is described as a 2 step polymerisation using poly(VDF-*co*-HFP) as seed material.

#### 5.1.2 Modification of poly(VDF-*co*-HFP) copolymer

Chapter 4 described the experimental procedure for modifying the commercial poly(VDF-*co*-HFP). The method of seeded emulsion polymerisation was used. The resulting latexes were characterised using the same analysis techniques that were used to characterise the commercial poly(VDF-*co*-HFP) in chapter 3. The modified latexes showed differences compared to the commercial poly(VDF-*co*-HFP) such as increased average particle size,

different flow characteristics (i.e. some latexes displayed shear thickening behaviour), higher surface tension, shifted melting and crystallisation temperatures. Lower density and viscosity was observed for latexes produced with more polar monomers. Particle size distribution showed an increased particle size for latexes 2-6 indicating either graft or core-shell morphology, however  $^{19}\text{F}$  NMR showed no modification of the VDF-HFP backbone. This suggests that the method of attachment of the monomers to the commercial poly(VDF-*co*-HFP) is mechanical rather than chemical. Peel tests showed no superior adhesion properties compared to the commercial poly(VDF-*co*-HFP) and film formation was observed at temperatures below  $25\text{ }^{\circ}\text{C}$ . Both observations are contradictory to claims made by Kato *et al* [49].

## 5.2 Suggestion for further work

Characterisation of the resultant latexes showed that the poly(VDF-*co*-HFP) copolymer backbone was not modified during the experiments. Further studies to determine the reaction mechanism and accurate chemical structure need to be done. SEM is proposed to confirm the core-shell morphology of the commercial poly(VDF-*co*-HFP) and modified latexes. Stability tests are also proposed to determine the lifetime of the modified latexes since separation of the samples was noticed after some time.

# References

- [1] J.G. Drobny. *Technology of Fluoropolymers*. CRC Press, Boca Raton, Florida, 2014. ISBN 9781420042672.
- [2] A.L. Allred. Electronegativity values from thermochemical data. *Journal of Inorganic and Nuclear Chemistry*, 17(3):215 – 221, 1961. ISSN 0022-1902.
- [3] Jack D. Dunitz. Organic fluorine: Odd man out. *ChemBioChem*, 5(5):614–621, 2004. doi: 10.1002/cbic.200300801. URL <https://onlinelibrary.wiley.com/doi/abs/10.1002/cbic.200300801>.
- [4] A. Bondi. van der waals volumes and radii. *The Journal of Physical Chemistry*, 68(3):441–451, 1964. doi: 10.1021/j100785a001. URL <https://doi.org/10.1021/j100785a001>.
- [5] V.C. Malshe and Nivedita S. Sangaj. Fluorinated acrylic copolymers: Part i: Study of clear coatings. *Progress in Organic Coatings*, 53(3):207 – 211, 2005. ISSN 0300-9440.
- [6] Elif Alyamac and Mark D. Soucek. Acrylate-based fluorinated copolymers for high-solids coatings. *Progress in Organic Coatings*, 71(3):213 – 224, 2011. ISSN 0300-9440.
- [7] J.M. DeSimone, Z. Guan, and C.S. Elsbernd. Synthesis of fluoropolymers in supercritical carbon dioxide. *Science*, 257(5072):945–947, 1992.
- [8] A.G. Pittman. Surface properties of fluorocarbon polymers. *Fluoropolymers*, 25, 1972.
- [9] B. Ameduri and B. Boutevin. Copolymerization of fluorinated monomers : recent developments and future trends. *Journal of Fluorine Chemistry*, 104:53–62, 2000.
- [10] John Scheirs. *Modern Fluoropolymers: High Performance Polymers for Diverse Applications*. Wiley, 1997.
- [11] Yanjun Chen, Chaocan Zhang, and Xinxin Chen. Emulsifier-free latex of fluorinated acrylate copolymer. *European Polymer Journal*, 42(3):694 – 701, 2006. ISSN 0014-3057.

- [12] Natanya M.L. Hansen, Katja Jankova, and Soren Hvilsted. Fluoropolymer materials and architectures prepared by controlled radical polymerizations. *European Polymer Journal*, 43(2):255 – 293, 2007. ISSN 0014-3057.
- [13] Bruno Ameduri and Bernard Boutevin. Chapter 1 - telomerisation reactions of fluorinated alkenes. In Bruno Ameduri and Bernard Boutevin, editors, *Well-Architected Fluoropolymers: Synthesis, Properties and Applications*, pages 1 – 99. Elsevier Science, Amsterdam, 2004. ISBN 978-0-08-044388-1.
- [14] Hongxiang Teng. Overview of the development of the fluoropolymer industry. *Applied Sciences*, 2:496–512, 2012.
- [15] He Ling and Liang Junyan. Synthesis, modification and characterization of core-shell fluoroacrylate copolymer latexes. *Journal of Fluorine Chemistry*, 129(7):590 – 597, 2008. ISSN 0022-1139.
- [16] J. Chen, S. Tan, G. Gao, H. Li, and Z. Zhang. Synthesis and characterization of thermally self curable fluoropolymer triggered by tempo in one pot for high performance rubber applications. *Polymer Chemistry*, 5:2130–2141, 2014.
- [17] S. Ebnesajjad. *Fluoroplastics, Volume 1: Non-melt Processible Fluoroplastics*. Elsevier Science, Norwich, New York, 2000. ISBN 9780815517276. URL <https://books.google.co.za/books?id=-H4yIE71aGMC>.
- [18] S. Ebnesajjad. *Fluoroplastics, Volume 2: Melt Processible Fluoroplastics: The Definitive User's Guide*. Elsevier Science, Norwich, New York, 2002. ISBN 9780815517283. URL [https://books.google.co.za/books?id=yJvZdv\\_S3-wC](https://books.google.co.za/books?id=yJvZdv_S3-wC).
- [19] S. Ebnesajjad. *Introduction to Fluoropolymers: Materials, Technology and Applications*. Elsevier Science, 2013. ISBN 9781455775514. URL <https://books.google.co.za/books?id=NrE7knXbDC0C>.
- [20] James Gardiner. Fluoropolymers: Origin, production, and industrial and commercial applications. *Australian Journal of Chemistry*, 68(1):13–22, 2015. doi: <https://doi.org/10.1071/CH14165>. URL <http://www.publish.csiro.au/paper/CH14165>.
- [21] B. Ameduri and H. Sawada. *Fluorinated Polymers: Volume 2: Applications*. Royal Society of Chemistry, 2016. ISBN 9781782629368.
- [22] S. Ebnesajjad. *Expanded PTFE Applications Handbook: Technology, Manufacturing and Applications*. Elsevier Science, Norwich, New York, 2016. ISBN 9781437778564. URL <https://books.google.fr/books?id=2veWaY0Q2ikC>.

- [23] Li-Piin Sung, Silvia Vicini, Derek L. Ho, Lotfi Hedhli, Christyn Olmstead, and Kurt A. Wood. Effect of microstructure of fluorinated acrylic coatings on UV degradation testing. *Polymer*, 45(19):6639 – 6646, 2004. ISSN 0032-3861.
- [24] Robert A. Iezzi, Scott Gaboury, and Kurt Wood. Acrylic-fluoropolymer mixtures and their use in coatings. *Progress in Organic Coatings*, 40(174):55 – 60, 2000. ISSN 0300-9440.
- [25] Sunee Wongchitphimon, Rong Wang, Ratana Jiraratananon, Lei Shi, and Chun Heng Loh. Effect of polyethylene glycol PEG as an additive on the fabrication of polyvinylidene fluoride-co-hexafluoropropylene (PVDF-HFP) asymmetric microporous hollow fiber membranes. *Journal of Membrane Science*, 369(1-2):329 – 338, 2011. ISSN 0376-7388.
- [26] Kurt A. Wood, Christopher Cypcar, and Lotfi Hedhli. Predicting the exterior durability of new fluoropolymer coatings. *Journal of Fluorine Chemistry*, 104(1):63 – 71, 2000. ISSN 0022-1139.
- [27] Kurt A. Wood. Optimizing the exterior durability of new fluoropolymer coatings. *Progress in Organic Coatings*, 43(173):207 – 213, 2001. ISSN 0300-9440. Athens 2000.
- [28] A. Bhattacharya and B.N. Misra. Grafting: a versatile means to modify polymers: Techniques, factors and applications. *Progress in Polymer Science*, 29(8):767 – 814, 2004. ISSN 0079-6700.
- [29] J. F. Hester, P. Banerjee, Y.Y. Won, A. Akthakul, M. H. Acar, and A. M. Mayes. Atrp of amphiphilic graft copolymers based on PVDF and their use as membrane additives. *Macromolecules*, 32:7652–7661, 2002.
- [30] A. Kuila, N. Maity, D.P. Chatterjee, and A.K. Nandi. Temperature triggered antifouling properties of poly(vinylidene fluoride) graft copolymers with tunable hydrophilicity. *Journal of Materials Chemistry A*, 3:13546–13555, 2015.
- [31] A. Kuila, D.P. Chatterjee, R.K. Layek, and A.K. Nandi. Coupled atom transfer radical coupling and atom transfer radical polymerization approach for controlled grafting from poly(vinylidene fluoride) backbone. *Journal of Polymer Science, Part A: Polymer Chemistry*, 52:995–1008, 2014.
- [32] M.-Cl. Clochard, J. Begue, A. Lafon, D. Caldemaïson, C. Bittencourt, J.-J. Pireaux, and N. Betz. Tailoring bulk and surface grafting of poly(acrylic acid) in electron-irradiated PVDF. *Polymer*, 45(26):8683 – 8694, 2004. ISSN 0032-3861.

- [33] Michael Friedman and Gerard Walsh. High performance films: Review of new materials and trends. *Polymer Engineering & Science*, 42(8):1756–1788, 2002. ISSN 1548-2634.
- [34] G.J. Wang, C.S. Kang, and R.G. Jin. Synthesis of acrylic core-shell composite polymers and properties of plastisol gels. *Progress in Organic Coatings*, 50(1):55 – 61, 2004. ISSN 0300-9440.
- [35] Christopher J. Ferguson, Gregory T. Russell, and Robert G. Gilbert. Synthesis of latices with polystyrene cores and poly(vinyl acetate) shells. 1. use of polystyrene seeds. *Polymer*, 43(24):6371 – 6382, 2002. ISSN 0032-3861.
- [36] Zhan-Min Wu, Wen-Zhong Zhai, Yu-Feng He, Peng-Fei Song, and Rong-Min Wang. Silicylacrylate copolymer core shell emulsion for humidity coatings. *Progress in Organic Coatings*, 77(11):1841 – 1847, 2014. ISSN 0300-9440.
- [37] Xuejun Cui, Shuangling Zhong, and Hongyan Wang. Synthesis and characterization of emulsifier-free core-shell fluorine-containing polyacrylate latex. *Colloids and Surfaces A: Physicochemical and Engineering Aspects*, 303(3):173 – 178, 2007. ISSN 0927-7757.
- [38] A.K. Khan, B.C. Ray, and S.K. Dolui. Preparation of core-shell emulsion polymer and optimization of shell composition with respect to opacity of paint film. *Progress in Organic Coatings*, 62(1):65 – 70, 2008. ISSN 0300-9440.
- [39] Jian-Zhong Ma, Yi-Hong Liu, Yan Bao, Jun li Liu, and Jing Zhang. Research advances in polymer emulsion based on "core-shell" structure particle design. *Advances in Colloid and Interface Science*, 197-198:118 – 131, 2013. ISSN 0001-8686.
- [40] Ping-Ting Xiong, De-Ping Lu, Pei-Zhi Chen, Hong-Zhi Huang, and Rong Guan. Preparation and surface properties of latexes with fluorine enriched in the shell by silicon monomer crosslinking. *European Polymer Journal*, 43(5):2117 – 2126, 2007. ISSN 0014-3057.
- [41] Jan-Erik Jonsson, Ola J. Karlsson, Helen Hassander, and Bertil Tornell. Semi-continuous emulsion polymerization of styrene in the presence of poly(methyl methacrylate) seed particles. polymerization conditions giving core-shell particles. *European Polymer Journal*, 43(4):1322 – 1332, 2007. ISSN 0014-3057.
- [42] L.A. Perez-Carrillo, M. Puca, M. Rabelero, K.E. Meza, J.E. Puig, E. Mendizabal, F. Lopez-Serrano, and R.G. Lopez. Effect of particle size on the mechanical properties of polystyrene and poly(butyl acrylate) core/shell polymers. *Polymer*, 48(5): 1212 – 1218, 2007. ISSN 0032-3861.

- [43] Akihiko Asakawa, Masao Unoki, Takao Hirono, and Takashi Takayanagi. Waterborne fluoropolymers for paint use. *Journal of Fluorine Chemistry*, 104(1):47 – 51, 2000. ISSN 0022-1139.
- [44] W. Darden. Environmentally friendly fluoropolymer resins for ultra-weatherable coatings. *PPCJ Polymers Paint Colour Journal*, 204(4593):20–26, 2014.
- [45] H. Lutz, H.-P. Weitzel, and W. Huster. 10.27 - aqueous emulsion polymers. In Krzysztof Matyjaszewski Martin Moller, editor, *Polymer Science: A Comprehensive Reference*, pages 479 – 518. Elsevier, Amsterdam, 2012. ISBN 978-0-08-087862-1.
- [46] Natasja A. Swartz, Kurt A. Wood, and Tami Lasseter Clare. Characterizing and improving performance properties of thin solid films produced by weatherable waterborne colloidal suspensions on bronze substrates. *Progress in Organic Coatings*, 75(3):215 – 223, 2012. ISSN 0300-9440.
- [47] Ines de F. A. Mariz, Ian S. Millichap, Jose C de la Cal, and Jose R. Leiza. High performance water-borne paints with high volume solids based on bimodal latexes. *Progress in Organic Coatings*, 68(3):225 – 233, 2010.
- [48] Yongshang Lu, Ying Xia, and Richard C. Larock. Surfactant-free core shell hybrid latexes from soybean oil-based waterborne polyurethanes and poly(styrene-butyl acrylate). *Progress in Organic Coatings*, 71(4):336 – 342, 2011. ISSN 0300-9440.
- [49] M Kato, T Hiraharu, K Nishiwaki, and H Tadenuma. Aqueous fluorine containing polymer dispersion and aqueous dispersion containing fluorine-containing polymer and water soluble resin and/or water dispersible resin, 1994. Patent, 1994, US 5349003.
- [50] A Earnshaw and N.N Greenwood. 17 - the halogens: Fluorine, chlorine, bromine, iodine and astatine. In N.N. Greenwood and A. Earnshaw, editors, *Chemistry of the Elements (Second Edition)*, pages 789 – 887. Butterworth-Heinemann, Oxford, second edition edition, 1984. ISBN 978-0-7506-3365-9.
- [51] J.I. Kroschwitz and A. Seidel. *Kirk-Othmer Encyclopedia of Chemical Technology*. Number v. 11 in Kirk-Othmer Encyclopedia of Chemical Technology. Wiley-Interscience, 2005. ISBN 9780471485124.
- [52] R.J Young and P.A Lovell. *Introduction to Polymers*. CRC Press, 2011.
- [53] Z.W. Wicks, F.N. Jones, S.P. Pappas, and D.A. Wicks. *Organic Coatings: Science and Technology*. Wiley, 2007. ISBN 9780470079065.

- [54] Zeno W. Wicks and Frank N. Jones. *Coatings*. John Wiley & Sons, Inc., 2000. ISBN 9780471238966.
- [55] L.W McKeen. *Fluorinated Coatings and Finishes - The Definitive User's Guide and Databook*. William Andrew Publishing, 2007.
- [56] Paula Hammond. 10.569 synthesis of polymers fall 2006 materials, April 2013. Massachusetts Institute of Technology.
- [57] Eduardo Vivaldo-lima, Philip E Wood, Archie E Hamielec, Alexander Penlidis, and Population Balance Equation. An updated review on suspension polymerization. *Ind. Eng. Chem. Res.*, 36(905):939–965, 1997.
- [58] B Ameduri. From vinylidene fluoride (vdf) to the applications of vdf-containing polymers and copolymers recent developments and future trends. *Chemical Reviews*, 109(12):6632–6686, 2009. ISSN 1520-6890.
- [59] C. Tournut. *Thermoplastic copolymers of vinylidene fluoride*, volume Modern Fluoropolymers: High Performance Polymers for Diverse Applications. John Wiley & Sons, Ltd., Chichester, New York, Weinheim, Brisbane, Singapore, Toronto, 1997.
- [60] Bruno Ameduri and Bernard Boutevin. Chapter 5 - synthesis, properties and applications of fluorinated graft copolymers. In Bruno Ameduri and Bernard Boutevin, editors, *Well-Architected Fluoropolymers: Synthesis, Properties and Applications*, pages 347 – 454. Elsevier Science, Amsterdam, 2004. ISBN 978-0-08-044388-1.
- [61] Xuejun Cui, Shuangling Zhong, and Hongyan Wang. Synthesis and characterization of emulsifier-free core-shell fluorine-containing polyacrylate latex. *Colloids and Surfaces A: Physicochemical and Engineering Aspects*, 303(3):173 – 178, 2007. ISSN 0927-7757.
- [62] H.A Barnes. Rheology of emulsions - a review. *Colloids and Surfaces A: Physicochemical and Engineering Aspects*, 91:89–95, 1994.
- [63] Th.F. Tadros. Fundamental principles of emulsion rheology and their applications. *Colloids and Surfaces A: Physicochemical and Engineering Aspects*, 91(0):39 – 55, 1994. ISSN 0927-7757.
- [64] J Drelich, Ch Fang, and CL White. Measurement of interfacial tension in fluid-fluid systems. *Encyclopedia of Surface and Colloid Science*, 3:3158–3163, 2002.
- [65] P.L. du Noüy. A new apparatus for measuring surface tension. *The journal of general physiology*, 5(1):521–524, 1919.

- [66] R. Macy. Surface tension by the ring method: Applicability of the du nouy apparatus. *Journal of Chemical Education*, pages 573–576, 1935.
- [67] Tharwat Tadros. Application of rheology for assessment and prediction of the long-term physical stability of emulsions. *Advances in Colloid and Interface Science*, 108-7109(0):227 – 258, 2004. ISSN 0001-8686.
- [68] Ludovic Dumas, Belen Albela, Laurent Bonneviot, Daniel Portinha, and Etienne Fleury. ESR investigation of radicals formed in  $\gamma$ -irradiated vinylidene fluoride based copolymer: P(VDF-co-HFP). *Radiation Physics and Chemistry*, 86:118 – 128, 2013. ISSN 0969-806X.
- [69] Tamer S. Ahmed, Joseph M. DeSimone, and George W. Roberts. Continuous copolymerization of vinylidene fluoride with hexafluoropropylene in supercritical carbon dioxide: Low hexafluoropropylene content semicrystalline copolymers. *Macromolecules*, 40:9322–9331, 2007.
- [70] Ye.M. Murasheva, A.S. Shashkov, and A.A. Dontsov. Analysis of the  $^{19}\text{F}$  NMR spectra of copolymers of vinylidene fluoride with tetrafluoroethylene, and of vinylidene fluoride with tetrafluoroethylene and hexafluoropropylene. The use of an empirical additive scheme and of the principle of alternation . *Polymer Science U.S.S.R.*, 23 (3):711 – 720, 1981. ISSN 0032-3950.
- [71] Maurizio Pianca, Piergiorgio Bonardelli, Marco Tato, Gianna Cirillo, and Giovanni Moggi. Composition and sequence distribution of vinylidene fluoride copolymer and terpolymer fluoroelastomers. Determination by  $^{19}\text{F}$  nuclear magnetic resonance spectroscopy and correlation with some properties. *Polymer*, 28(2):224 – 230, 1987. ISSN 0032-3861.
- [72] Amr I. Abdel-Fattah, Mohamed S. El-Genk, and Paul W. Reimus. On visualization of sub-micron particles with dark-field light microscopy. *Journal of Colloid and Interface Science*, 246(2):410 – 412, 2002. ISSN 0021-9797.
- [73] Y. Zhang, Rui Zhang, C. Yang, Jing Xu, Jian Zheng, and M. Lu. Stable acrylate/triethoxyvinylsilane VTES core-shell emulsion with low surface tension made by modified micro-emulsion polymerization: Effect of different mass ratio of MMA/BA in the core and shell. *Colloids and Surfaces A: Physicochemical and Engineering Aspects*, 436:549 – 556, 2013. ISSN 0927-7757.
- [74] O.S.R. Liz, A.S. Medeiros, and L.O. Faria. FTIR and DSC studies on gamma irradiated P(VdF-HFP) fluoropolymers applied to dosimetry. *Nuclear Instruments and Methods in Physics Research Section B: Beam Interactions with Materials and Atoms*, 269(23):2819 – 2823, 2011. ISSN 0168-583X.

- [75] American Society for Testing and Materials. Standard test methods for measuring adhesion by tape test. *ASTM D3359-09*, 2010.
- [76] M.P. Gellin and B. Ameduri. Radical solution copolymerization of vinylidene fluoroide with hexafluoropropene. *Journal of Fluorine Chemistry*, 126:577–585, 2005.
- [77] Eric B. Twum, Chun Gao, Xiaohong Li, Elizabeth F. McCord, Peter A. Fox, Donald F. Lyons, and Peter L. Rinaldi. Characterization of the chain-ends and branching structures in polyvinylidene fluoride with multidimensional NMR. *Macromolecules*, 45(13):5501–5512, 2012.
- [78] Stephen J. Blanksby and G. Barney Ellison. Bond dissociation energies of organic molecules. *Accounts of Chemical Research*, 36(4):255–263, 2003. doi: 10.1021/ar020230d.
- [79] W. H. Yu, E. T. Kang, and K. G. Neoh. Controlled grafting of comb copolymer brushes on poly(tetrafluoroethylene) films by surface-initiated living radical polymerizations. *Langmuir*, 21(1):450–456, 2005. doi: 10.1021/la0485531.
- [80] El-Sayed A. Hegazy, Isao Ishigaki, and Jiro Okamoto. Radiation grafting of acrylic acid onto fluorine-containing polymers. i. kinetic study of preirradiation grafting onto poly(tetrafluoroethylene). *Journal of Applied Polymer Science*, 26(9):3117–3124, 1981. doi: 10.1002/app.1981.070260925.
- [81] Jingyi Qiu, Jiangfeng Ni, Maolin Zhai, Jing Peng, Henghui Zhou, Jiuqiang Li, and Genshuan Wei. Radiation grafting of styrene and maleic anhydride onto ptfе membranes and sequent sulfonation for applications of vanadium redox battery. *Radiation Physics and Chemistry*, 76(11):1703–1707, 2007.
- [82] Chen Wang and Jie-Rong Chen. Studies on surface graft polymerization of acrylic acid onto ptfе film by remote argon plasma initiation. *Applied Surface Science*, 253(10):4599–4606, 2007.